Smad4 is dispensable for normal pancreas development yet critical in progression and tumor biology of pancreas cancer

Nabeel Bardeesy,[1,7,8] Kuang-hung Cheng,[1,7] Justin H. Berger,[1] Gerald C. Chu,[2,3] Jessica Pahler,[4] Peter Olson,[4] Aram F. Hezel,[1,3] James Horner,[2,3] Gregory Y. Lauwers,[5] Douglas Hanahan,[4] and Ronald A. DePinho[2,3,6,9]

[1]Massachusetts General Hospital Cancer Center and Department of Medicine, Harvard Medical School, Boston, Massachusetts 02115, USA; [2]Center for Applied Cancer Science, Belfer Foundation Institute for Innovative Cancer Science, Dana-Farber Cancer Institute, Boston, Massachusetts 02115, USA; [3]Department of Medical Oncology, Dana-Farber Cancer Institute, Boston, Massachusetts 02115, USA; [4]Department of Biochemistry and Biophysics, Comprehensive Cancer Center, and Diabetes Center, University of California at San Francisco, San Francisco, California 94143, USA; [5]Gastrointestinal Pathology Service, Department of Pathology, Massachusetts General Hospital and Harvard Medical School, Boston, Massachusetts 02115, USA; [6]Department of Medicine and Genetics, Harvard Medical School, Boston, Massachusetts 02115, USA

***SMAD4* is inactivated in the majority of pancreatic ductal adenocarcinomas (PDAC) with concurrent mutational inactivation of the *INK4A/ARF* tumor suppressor locus and activation of the *KRAS* oncogene. Here, using genetically engineered mice, we determined the impact of *SMAD4* deficiency on the development of the pancreas and on the initiation and/or progression of PDAC—alone or in combination with PDAC-relevant mutations. Selective *SMAD4* deletion in the pancreatic epithelium had no discernable impact on pancreatic development or physiology. However, when combined with the activated $KRAS^{G12D}$ allele, *SMAD4* deficiency enabled rapid progression of $KRAS^{G12D}$-initiated neoplasms. While $KRAS^{G12D}$ alone elicited premalignant pancreatic intraepithelial neoplasia (PanIN) that progressed slowly to carcinoma, the combination of $KRAS^{G12D}$ and *SMAD4* deficiency resulted in the rapid development of tumors resembling intraductal papillary mucinous neoplasia (IPMN), a precursor to PDAC in humans. *SMAD4* deficiency also accelerated PDAC development of $KRAS^{G12D}$ *INK4A/ARF* heterozygous mice and altered the tumor phenotype; while tumors with intact *SMAD4* frequently exhibited epithelial-to-mesenchymal transition (EMT), PDAC null for *SMAD4* retained a differentiated histopathology with increased expression of epithelial markers. *SMAD4* status in PDAC cell lines was associated with differential responses to transforming growth factor-β (TGF-β) in vitro with a subset of SMAD4 wild-type lines showing prominent TGF-β-induced proliferation and migration. These results provide genetic confirmation that *SMAD4* is a PDAC tumor suppressor, functioning to block the progression of $KRAS^{G12D}$-initiated neoplasms, whereas in a subset of advanced tumors, intact *SMAD4* facilitates EMT and TGF-β-dependent growth.**

[*Keywords*: Smad4; pancreatic cancer; epithelial-to-mesenchymal transition mouse models; TGF-β]

Supplemental material is available at http://www.genesdev.org.

Received August 4, 2006; revised version accepted September 14, 2006.

PDAC (pancreatic ductal adenocarcinoma) ranks as the fourth leading cause of cancer mortality in the United States and carries a median survival of <6 mo (Li et al. 2004). Hallmarks of this disease include the infiltration of the tumor with a proliferative stroma (desmoplasia), early invasion and metastasis, and pronounced genomic instability (Solcia et al. 1995). PDAC is characterized by a highly recurrent pattern of genetic lesions consisting of activating mutations of *KRAS* and inactivation of *INK4A* (via mutation, deletion, or promoter methylation) in virtually all cases, inactivation of the p53–ARF pathway in ~87% of cases (including tumors with deletions of the *INK4A/ARF* locus), and *SMAD4* inactivation in ~53% (Hansel et al. 2003). Hence, *SMAD4* status can be considered as a distinguishing molecular feature of two major classes of PDAC. Significant ongoing efforts are being directed toward the elucidation of how specific signature mutations contribute to the genesis and progression of PDAC and influence its tumor biological features.

[7]**These authors contributed equally to this work.**
Corresponding authors.
[8]**E-MAIL nelbardeesy@partners.org; FAX (617) 643-3170.**
[9]**E-MAIL Ron_depinho@dfci.harvard.edu; FAX (617) 632-6069.**
Article is online at http://www.genesdev.org/cgi/doi/10.1101/gad.1478706.

Morphological and genetic analyses have implicated three distinct ductal neoplasms as potential precursor lesions of human PDAC, designated pancreatic intraepithelial neoplasms (PanIN), intraductal papillary mucinous neoplasms (IPMN), and mucinous cystic neoplasms (MCN) (Maitra et al. 2005). The best characterized of these neoplasms, PanIN, appears to evolve in a stepwise manner through stages that display increasing cellular atypia and accumulating clonal mutations—in *KRAS*, $p16^{INK4A}$, $p14^{ARF}$, *p53*, and *SMAD4*—in the course of progressing to PDAC (Hansel et al. 2003). IPMN and MCN—distinguished by their cystic character—show a comparable mutational profile to PanIN, albeit with different frequencies of the various mutations. The interrelationship of these various premalignant neoplasms and the basis for these tumor phenotypes are not clear.

Genetically engineered mouse models have provided a system to define genotype–phenotype relationships in PDAC pathobiology. In the mouse pancreas, expression of an activated Kras ($Kras^{G12D}$) knock-in allele induces PanIN lesions that can gradually progress to PDAC (average latency >1 yr) (Aguirre et al. 2003; Hingorani et al. 2003). Inactivation of the *Ink4a/Arf* tumor suppressor locus (encoding both $p16^{INK4A}$ and $p19^{ARF}$), or of *p53*, does not induce pancreatic neoplasia; however, concurrent $Kras^{G12D}$ expression and inactivation of *Ink4a/Arf* or *p53* drives the development of advanced PDAC with short latency (Aguirre et al. 2003; Hingorani et al. 2005; Bardeesy et al. 2006). The role of *Smad4* has not yet been investigated in the context of these models. Mice with germline homozygous *Smad4* inactivation die during early embryogenesis, while $Smad4^{+/-}$ mice develop gastric and duodenal polyps but have not been reported to have pancreatic pathology (Sirard et al. 1998; Yang et al. 1998; Takaku et al. 1999).

Inactivating mutations in *SMAD4* are far more common in PDAC than in other cancer types (Hahn et al. 1996). This tumor suppressor gene encodes a transcription factor that is a central effector of the transforming growth factor-β (TGF-β), bone morphogenetic protein (BMP), and Activin signaling pathways (Bierie and Moses 2006). TGF-β, BMP, or Activin family ligands signal through cognate receptor serine/threonine kinases that phosphorylate receptor SMADs—SMAD1, SMAD2, SMAD3, SMAD5, and SMAD8. The activated receptor SMADs bind to SMAD4 and translocate to the nucleus, where higher-order transcriptional complexes regulate expression of broad sets of genes. These pathways can also signal independently of SMAD4 as reflected by the capacity of TGF-β to regulate JNK and Par6 in some cell types and to induce Smad2/3-TIF1γ transcriptional complexes (He et al. 2006; for review, see Bierie and Moses 2006).

TGF-β is a potent inhibitor of epithelial cell growth and survival through modulation of expression of cell cycle regulators and activation of apoptosis, although these effects are highly dependent on cellular context (Bierie and Moses 2006). The tumor suppressor role of TGF-β signaling is underscored by presence of inactivating TGF-β receptor mutations in several cancers. On the other hand, TGF-β can enhance the malignant growth of some established epithelial tumors, promoting tumor cell proliferation, migration, and the epithelial-to-mesenchymal transition (EMT)—a process by which advanced carcinomas acquire a highly invasive, undifferentiated and metastatic phenotype (Zavadil and Bottinger 2005). Therefore, TGF-β signaling can have biphasic stage-specific effects—inhibiting carcinoma initiation while promoting the high-grade advancement and dissemination of established tumors. BMP signaling also has a clear role in tumorigenesis as demonstrated by the association of juvenile polyposis syndrome with germline loss-of-function mutations in either *BMPR-1A* or in *SMAD4* (Howe et al. 1998, 2001); the impact of these germline mutations on PDAC risk or clinical presentation is not defined.

The biological role of *SMAD4* mutations in human PDAC progression is an area of active investigation, often with contrasting observations. PDAC cell lines show variable sensitivity to TGF-β-induced cytotoxicity in a manner that appears independent of *SMAD4* status (Dai et al. 1999; Giehl et al. 2000; Jonson et al. 2003; Nicolas and Hill 2003; Subramanian et al. 2004). Some evidence suggests that a prominent role for SMAD4 resides in modulating the tumor microenvironment. Specifically, while *SMAD4* restoration in some PDAC cell lines has minimal effects on cell growth in vitro, there is strong inhibition of PDAC xenografts perhaps through repression of angiogenesis and extracellular matrix remodeling (Schwarte-Waldhoff et al. 2000; Duda et al. 2003). On the other hand, separate studies have shown that *SMAD4* restoration results in attenuated growth in soft agar of some PDAC cell lines, suggesting a cell-autonomous function (Peng et al. 2002).

Complicating interpretation of the role of *SMAD4* loss in PDAC is the observation that TGF-β signaling may enhance tumorigenicity in established tumors. TGF-β ligands and receptors are frequently expressed at elevated levels in PDAC relative to normal pancreas, and this overexpression appears to correlate with decreased survival (Friess et al. 1993b; Wagner et al. 1999). TGF-β is thought to promote PDAC desmoplasia as well as contribute to proliferation of the tumor cells in an autocrine manner (Friess et al. 1993a; Wagner et al. 1999; Lohr et al. 2001); notably, blockade of TGF-β signaling by expression of soluble type II TGF-β receptor attenuates tumorigenicity of xenografts (Rowland-Goldsmith et al. 2001), and, reciprocally, exogenous addition of TGF-β enhances tumor invasion (Ellenrieder et al. 2001).

It is notable that opposing conclusions have been reached, in separate clinicopathological studies, regarding the impact of *SMAD4* status on the prognosis of PDAC. One study determined that patients expressing SMAD4 had significantly worse outcomes and did not benefit from surgery (Tascilar et al. 2001), while another study indicated that SMAD4 expression predicted increased survival and improved response to surgery (Biankin et al. 2002). Overall, the complex response profiles to TGF-β suggest that TGF-β/SMAD4 signaling may

have pleiotropic and context-dependent roles in PDAC. This significant genetic and biological complexity provides formidable challenges in designing therapeutic strategies directed against this pathway. In this study, we sought to understand the role of *Smad4* in normal pancreas development and physiology as well as in the genesis and progression of PDAC, alone or together with other common PDAC genetic lesions.

Results

Normal development and function of the SMAD4-deficient pancreas

To study the role of *Smad4* in pancreatic development, physiology, and malignant transformation, we generated a conditional knockout allele of *Smad4* (*Smad4^{lox}*) harboring *loxP* sites flanking exons 8 and 9 in the mouse germline (Fig. 1A). We crossed *Smad4^{lox}* homozygous mice to either the *Pdx1-Cre* or *Ptf1a-Cre* transgenic mice (Gu et al. 2002; Kawaguchi et al. 2002) (hereafter, for brevity, *Cre* will be used for references to both strains together); these transgenes direct Cre recombinase expression to the epithelial lineages of the embryonic pancreas (*Pdx1-Cre* is also expressed in the duodenum and pylorus). The use of *Pdx1-Cre* allowed direct comparison with our existing extensively characterized *Pdx1-Cre*-driven models of PDAC, while the more organ-specific *Ptf1a-Cre* transgene obviated certain extra-pancreatic phenotypes (see below). Cre-mediated rearrangement of the *Smad4^{lox}* locus in pancreas tissue from *Cre Smad4$^{lox/lox}$* mice was documented by allele-specific PCR genotyping (data not shown) and by elimination of Smad4 protein on Western blot analysis (Fig. 1B), confirming generation of a null allele in the pancreas.

Mice with homozygous deletion of *Smad4* in the pancreas were born at the expected frequency (data not shown), showed no evidence of any gross anatomic or physiological abnormalities, and exhibited normal pancreatic cytoarchitecture and differentiation throughout

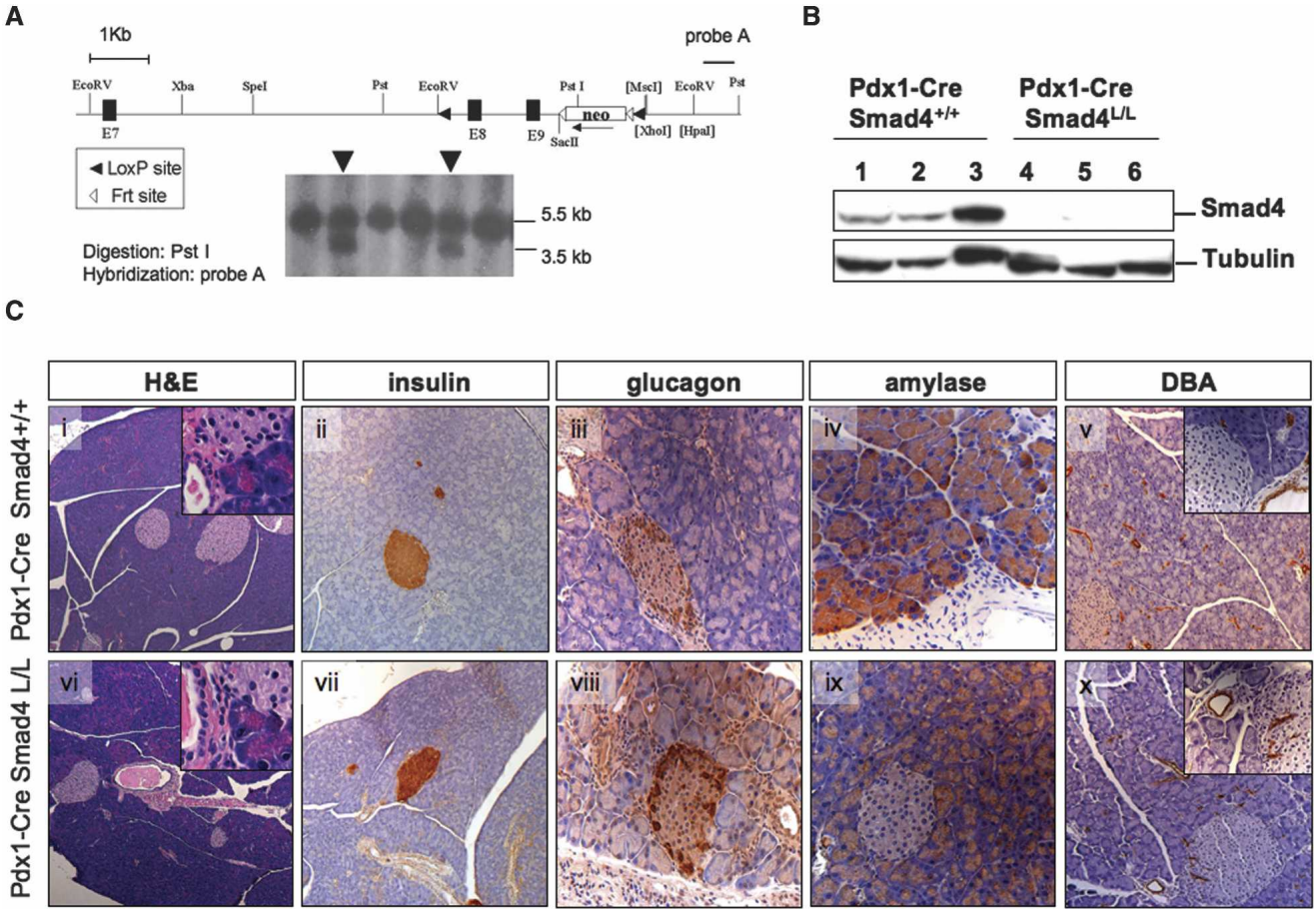

Figure 1. Conditional deletion of *Smad4* in the pancreas. (*A*, *top*) Genomic structure of the targeted *Smad4* allele. Exons (black rectangles), the Pgk-Neo cassette, loxP sites, Frt sites, and the probe for embryonic stem (ES) cell screening (black bar) are depicted. (*Bottom*) Southern blot of targeted *Smad*4 locus in two ES cell clones (arrowheads). (*B*) Western blot analysis of Smad4 expression in pancreatic lysates from 8-wk-old *Pdx1-Cre Smad4$^{+/+}$* and *Pdx1-Cre Smad4$^{lox/lox}$* mice. (*C*) Histological sections from 8-wk-old *Pdx1-Cre Smad4$^{+/+}$* (panels *i–v*) and *Pdx1-Cre Smad4$^{lox/lox}$* (panels *vi–x*) mice stained with H&E (panels *i*,*vi*); with antibodies to insulin (panels *ii*,*vii*), glucagon (panels *iii*,*viii*), and amylase (panels *iv*,*ix*); and with DBA-lectin (panels *v*,*x*). Magnifications: Panels *i*,*vi*, 50×; panels *ii*,*v*,*vii*,*x*, 100×; panels *iii*,*iv*,*viii*,*ix*, and *insets*, panels *v*,*x*, 200×; *insets*, panels *i*,*vi*, 400×.

postnatal life (n = 10 mice, ages 46–70 wk) (Fig. 1C). In addition, the normal glucose tolerance tests and normal serum lipase and amylase levels at 10 wk of age were consistent with the generally healthy appearance and weight gain of these mice. Amylase, insulin, and glucagon showed normal expression by immunohistochemical analysis, and staining with the *Dolichos biflorus* (DBA) lectin confirmed the presence of a normal proportion of pancreatic ducts (Fig. 1C). Finally, it is notable that none of the *Cre Smad4$^{lox/lox}$* animals developed pancreatic neoplasms (up to 70 wk of age/observation), although all *Pdx1-Cre Smad4$^{lox/lox}$* mice were found to harbor duodenal polyps comparable to those previously reported in germline *Smad4$^{+/-}$* mice (Takaku et al. 1999; Supplementary Fig. 1A). These data indicate that *Smad4* inactivation alone does not prominently affect pancreas development or physiology or play a role in the initiation of pancreatic cancer (see Discussion).

Kras^{G12D}-directed pancreatic tumorigenesis is enhanced in mice with Smad4 deletion

To investigate the role of *Smad4* in regulating PDAC progression, we first studied the activation state of TGF-β family signaling throughout the course of tumorigenesis in the *Pdx1-Cre LSL-Kras^{G12D}* model. We found that expression of TGF-β1 and BMP4 were induced in the PanINs and metaplastic ducts of *Pdx1-Cre LSL-Kras^{G12D}* pancreata as demonstrated by immunohistochemical analysis (Fig. 2A,B). Moreover, we detected nuclear localization of Smad2/3 in PanIN lesions by immunofluorescence (Fig. 2C), and Smad2 phosphorylation was revealed by immunoblot analysis (Fig. 2D). RT–PCR analysis confirmed the induction and sustained expression of TGF-β, and BMP4 in PanIN and established PDAC (Fig. 2E); moreover, expression profiling analysis of PDAC samples demonstrated broad induction of TGF-β pathway components (Supplementary Fig. 2). These data indicate that TGF-β signaling is activated in PanINs and advanced cancers, consistent with observations in human specimens (Friess et al. 1993b; Wagner et al. 1999; Ito et al. 2004), suggesting that this signaling pathway may serve to support neoplastic growth in the pancreas or, alternatively, provide a checkpoint mechanism designed to constrain tumor progression.

Molecular studies have identified distinct subsets of human PDAC that have common mutations in *KRAS* and *INK4A* and are distinguished by intact or loss-of-function alleles of *SMAD4*. These mutational profiles, coupled with the activated TGF-β signaling in *Kras^{G12D}*-induced PanINs, prompted evaluation of mice harboring various combinations of *Cre*, *LSL-Kras^{G12D}*, *Smad4^{lox}*, and/or *Ink4a/Arf^{lox}* alleles. As reported previously, *Cre*-mediated activation of the *LSL-Kras^{G12D}* allele in the pancreas resulted in the development of slowly progressive PanINs with uniformly good health through age 40 wk and thereafter a subset of these mice developed PDAC (Aguirre et al. 2003; Hingorani et al. 2003; Bardeesy et al. 2006). In contrast, the combination of activated *Kras^{G12D}* and *Smad4* deficiency resulted in a dramatic reduction in survival; all *Ptf1a-Cre LSL-Kras^{G12D} Smad4$^{lox/lox}$* (n = 7) and *Pdx1-Cre LSL-Kras^{G12D} Smad4$^{lox/lox}$* (n = 8) mice presented with a palpable abdominal mass between ages 7 and 12 wk, and reached terminal morbidity between ages 8 and 24 wk of age ($p < 0.001$ for both colonies compared with *Pdx1-Cre LSL-Kras^{G12D}* cohort) (Fig. 3A; Table 1).

Gross inspection of the *Ptf1a-Cre LSL-Kras^{G12D} Smad4$^{lox/lox}$* mice at necropsy revealed cystic pancreata in 12 of 12 cases (Fig. 3B). Comparable pancreatic tumors were observed in five out of eight *Pdx1-Cre LSL-Kras^{G12D} Smad4$^{lox/lox}$* mice with five out of eight of these mice also possessing gastric tumors, consistent with foregut expression of *Pdx1* (Supplementary Fig. 1B). Histological analysis revealed large lesions reminiscent of increasing grades of human IPMN in 17 out of 20 mice (Fig. 3C–E), while PDAC with papillary and moderately differentiated ductal elements was observed in two out of 20 mice (Fig. 3F; see Table 1). Pancreatic ductal neoplasms in humans show characteristic profiles of mucin expression (Moniaux et al. 2004); assessment of the murine IPMNs revealed positive staining for Muc1, Muc4, and Muc5AC and absence of reactivity for Muc2 and Cdx2, indicating that the mouse lesions resemble the "gastric-type" IPMN in humans (Fig. 3G–I; Adsay et al. 2004). The stomach cancers in the *Pdx1-Cre* mice showed either squamous or adenosquamous histology (Supplementary Fig. 1B). Together, our findings provide clear genetic evidence of a role of *Smad4* in blocking the progression of Kras^{G12D}-initiated PanINs to lethal pancreatic and gastric cancer.

We have reported previously on the absence of pancreatic neoplasia in *Pdx1-Cre Ink4a/Arf* mutant mice (Aguirre et al. 2003). Extending those results, we observed only a modest cancer predisposition in the *Pdx1-Cre Smad4$^{lox/lox}$ Ink4a/Arf$^{lox/lox}$* or *Pdx1-Cre Smad4$^{lox/lox}$ Ink4a/Arf$^{lox/+}$* mice. Examination of 23 mice, ages 30 and 64 wk, revealed a single case of an IPMN-like tumor and another with metastatic gastric cancer (Table 1). Thus, these observations underscore the roles of these tumor suppressors in progression rather than initiation of pancreatic cancer, as well as the requirement of coincident activated Kras signaling in order to effect malignant transformation.

Smad4 deficiency enhances development of Kras^{G12D}-initiated pancreatic ductal lesions

The more rapid tumor progression in mice with combined *Kras^{G12D}* activation and *Smad4* deficiency prompted more detailed cellular and molecular analyses to clarify the impact of *Smad4* deletion on evolving pancreatic neoplasms in the *Kras^{G12D}* model. In previous studies, the *Pdx1-Cre LSL-Kras^{G12D}* mice developed focal PanINs by 3 wk that showed a gradual increase in size and number but no malignant progression over the next 20 wk (Aguirre et al. 2003; Hingorani et al. 2003). On the basis of these kinetics, we performed serial autopsies at 2, 4, 5, and 8 wk (n = 3–8 mice per time point). While no histological differences were evident at 2 wk

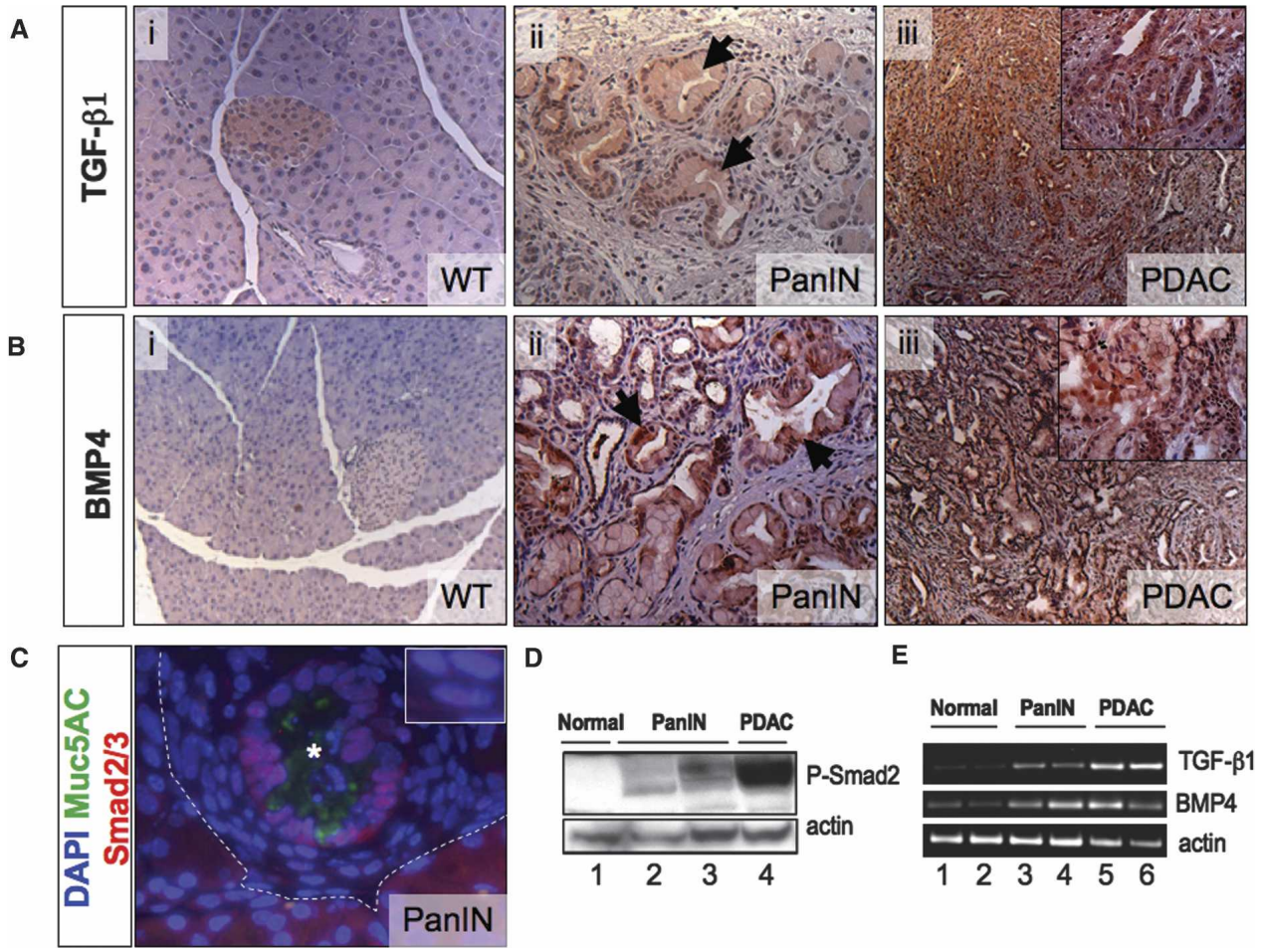

Figure 2. TGF-β family signaling in $Kras^{G12D}$-initiated PanIN/PDAC. Immunohistochemical staining for TGF-β (*A*) and BMP-4 (*B*) in pancreata from wild-type mice (panel *i*), *Pdx1-Cre LSL-Kras*^{G12D} mice (panel *ii*), and *Pdx1-Cre LSL-Kras*^{G12D} *Ink4a/Arf*$^{lox/lox}$ mice (panel *iii*) with PDAC. Note positive staining for both TGF-β and BMP4 in normal islets (panel *i*), in PanINs and metaplastic ducts (panel *ii*), and in PDAC (panel *iii*). (*C*) Immunofluorescence staining for Smad2/3 (red) and Muc5ac (green) in a PanIN arising in a *Pdx1-Cre LSL-Kras*^{G12D} mouse (region *above* dashed line; the PanIN lumen is marked with an asterisk). The ductal epithelial cells of the PanIN show cytoplasmic and membranous Muc5ac staining and nuclear localization of Smad2/3. (*Inset*) The stromal cells surrounding the PanIN epithelium also show nuclear Smad2/3. Nuclei are stained with DAPI (blue). (*D*) Western blot showing expression of phospho-Smad2/3 in a pancreas from a wild-type mouse (lane *1*), from *Pdx1-Cre LSL-Kras*^{G12D} mice (lanes *2*,*3*), and in PDAC from a *Pdx1-Cre LSL-Kras*^{G12D} *Ink4a/Arf*$^{lox/lox}$ mouse (lane *4*). (*E*) RT–PCR analysis of TGF-β1, BMP4, and actin expression in pancreata from wild-type mice (lanes *1*,*2*), *Pdx1-Cre LSL-Kras*^{G12D} mice (lanes *3*,*4*), and in PDAC from *Pdx1-Cre LSL-Kras*^{G12D} *Ink4a/Arf*$^{lox/lox}$ mice (lanes *5*,*6*). Magnifications: *A* (panels *i*,*iii*), *B* (panels *i*,*iii*), 100×; *A* (panels *ii*,*iii* [*inset*]), *B* (panels *ii*,*iii* [*inset*]), 200×; *C*, 630×.

(data not shown), the 4-wk time point revealed a significant impact of *Smad4* deficiency. Although age-matched *Cre LSL-Kras*^{G12D} and *Cre LSL-Kras*^{G12D} *Smad4*$^{lox/lox}$ pancreata (n = 6 mice/genotype) both showed low-grade PanINs and acinar-ductal metaplasia, *Smad4* deficiency correlated with a significant increase in both the number and size of the lesions (p = 0.004 and p = 0.01, respectively; Mann-Whitney), as demonstrated by morphometric analysis (Fig. 4A [panels i,v], B; see Materials and Methods). These more pronounced pathological changes were associated with rapid neoplastic progression in the *Ptf1-Cre LSL-Kras*^{G12D} *Smad4*$^{lox/lox}$ animals, which showed extensive IPMN and advanced PanIN lesions by 8 wk, whereas their age-matched *Ptf1-Cre LSL-Kras*^{G12D} counterparts had only focal low-grade PanINs (Fig. 4C).

We next sought to characterize potential *Smad4*-dependent changes in the neoplastic epithelium and in the tumor microenvironment. IHC analysis of lesions at 4 wk in both genotypes revealed comparably altered epithelial differentiation and activation of early developmental pathways implicated in PDAC development, with positive staining for cytokeratin-19; Shh1; Hes1; Pdx1; phospho-Stat3;mucins Muc1, Muc4, and Muc5AC; and lack of acinar (amylase) and islet (insulin) marker expression (Fig. 4A; Supplementary Table 1; Moniaux et al. 2004; Hezel et al. 2006; data not shown).

On the other hand, the PanIN and metaplastic ductal lesions in *Cre LSL-Kras*^{G12D} *Smad4*$^{lox/lox}$ mice demonstrated increased proliferation relative to lesions in *Cre LSL-Kras*^{G12D} *Smad4*$^{+/+}$ mice and to controls, with

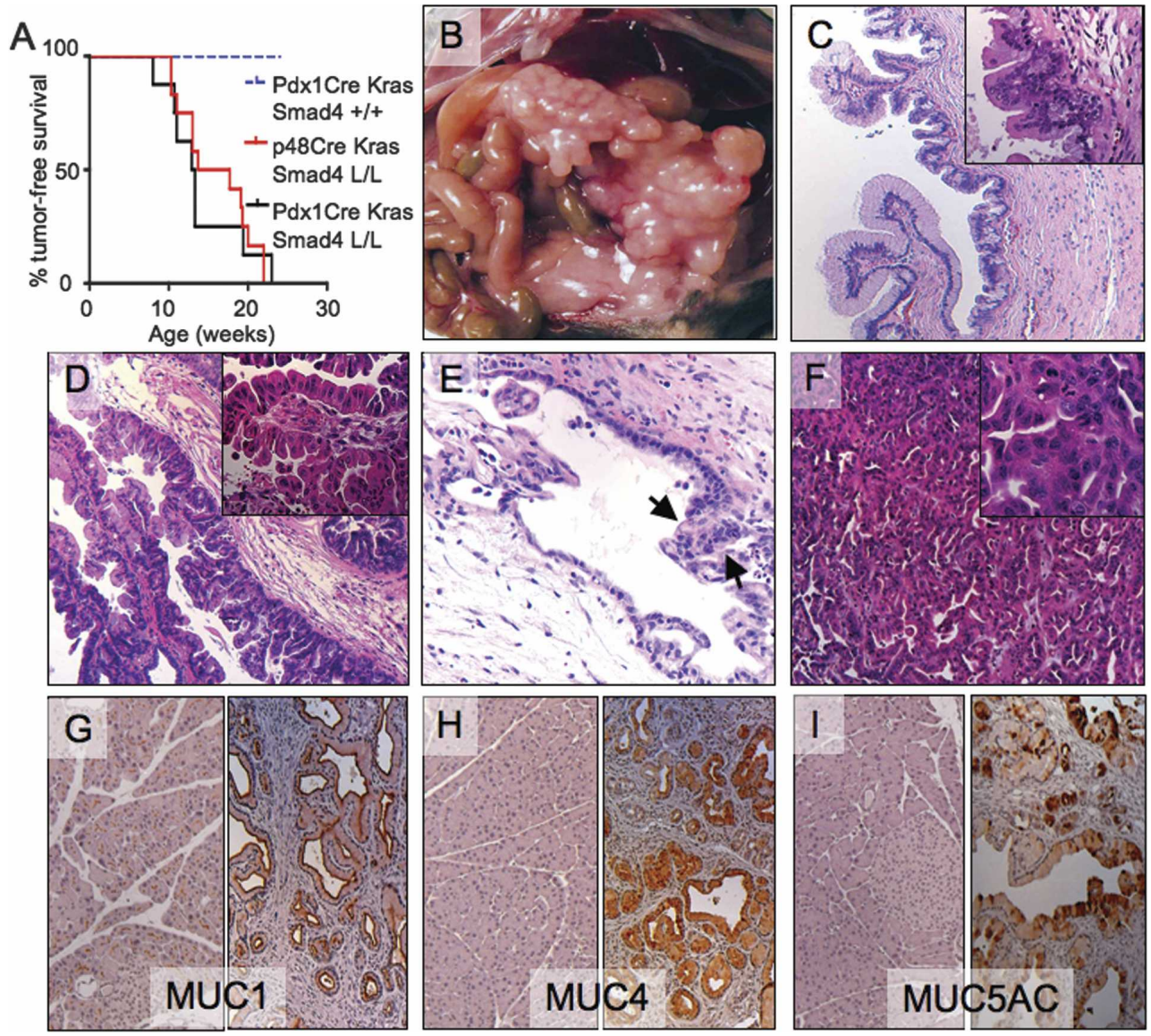

Figure 3. *Smad4* suppresses $Kras^{G12D}$-driven pancreatic tumorigenesis. (*A*) Survival curve (Kaplan-Meier) of the *Pdx1-Cre LSL-*$Kras^{G12D}$, *Ptf1a-Cre LSL-*$Kras^{G12D}$ $Smad4^{lox/lox}$, and *Pdx1-Cre LSL-*$Kras^{G12D}$ $Smad4^{lox/lox}$ cohorts. (*B–I*) Pancreatic tumorigenesis in *Ptf1a-Cre LSL-*$Kras^{G12D}$ $Smad4^{lox/lox}$ mice. (*B*) Gross photo of cystic pancreatic tumor in a 14-wk-old mouse. *C* and *D* show H&E images of the pancreas in *B* demonstrating regions of IPMN adenoma (*C*), borderline IPMN (*D*), and IPMN with carcinoma (*E*) in situ (arrows). (*F*) H&E image from 17-wk-old mouse showing PDAC with moderately differentiated ductal histology. (*G–I*) IHC of normal pancreas (*left* panels) and IPMN (*right* panels) staining for Muc1 (*G*), Muc4 (*H*), and Muc5AC (*I*). Magnifications: *C–I*, 100×; *C* (*inset*), 200×; *insets* in *E*,*F*, 400×.

prominent BrdU staining in both epithelial and stromal cells (Fig. 5A). Desmoplasia, a hallmark of PDAC in humans (Solcia et al. 1995), is a collagen-rich stromal proliferation within a tumor containing proliferative fibroblasts including so-called pancreatic stellate cells that have been implicated in promotion of tumorigenesis (Apte et al. 2004). In the normal pancreas, collagen-1 expression marks the periacinar and periductal fibroblasts (Fig. 5B). Multilabel immunofluorescence and BrdU staining was used to assess both the extent of stromal deposition and the relative rates of proliferation in the fibroblast and ductal epithelial compartments (detected by collagen-1 and DBA lectin immunofluorescence, respectively). In 4-wk old mice, the ductal lesions from both models expressed collagen 1 in their stroma, with the staining being particularly prominent in the larger lesions in the *Smad4*-deficient animals (Fig. 5C); quantitation of the BrdU staining confirmed that *Smad4* deficiency was associated with significantly increased proliferation of both the neoplastic epithelium and the associated stromal fibroblasts ($p < 0.001$, unpaired *t*-test) (Fig. 5D).

Activated stellate cells in human PDAC are characterized by induction of expression of smooth muscle actin

Table 1. *Mouse tumor phenotypes*

Genotype	Tumor-free survival (wk)	IPMN	PDAC	Gastric cancer
Pdx1-Cre Smad4 L/L	>52	0/10	0/10	0/10
Pdx1-Cre Ink4a/Arf L/+ Smad4 L/L	>52	1/10	0/10	0/10
Pdx1-Cre Ink4a/Arf L/L Smad4 L/L	>52	0/12	0/12	1/12
(Pdx1-Cre or Ptf1a-Cre) KrasG12D	>52	0/9	2/9	0/9
Ptf1a-Cre $Kras^{G12D}$ Smad4 L/L	15.7	12/12	2/12	0/12
Pdx1-Cre $Kras^{G12D}$ Smad4 L/L	13.1	5/8	0/8	5/8
(Pdx1-Cre or Ptf1a-Cre) KrasG12D Ink4a/Arf L/+	38	0/10	6/10	0/10
Ptf1a-Cre KrasG12D Ink4a/Arf L/+ Smad4 L/L	14	5/13	12/13	0/13
Pdx1-Cre KrasG12D Ink4a/Arf L/+ Smad4 L/L	12.6	4/12	4/12	8/12
(Pdx1-Cre or Ptf1a-Cre) KrasG12D Ink4a/Arf L/L	8.6	0/6	6/6	0/6
Ptf1a-Cre KrasG12D Ink4a/Arf L/L Smad4 L/L	8.8	0/4	4/4	0/4
Pdx1-Cre KrasG12D Ink4a/Arf L/L Smad4 L/L	7.4	3/10	9/10	5/10

expression (SMA), vimentin, and PDGFRβ (Apte et al. 2004). Further characterization of the fibroblast compartment revealed comparable marker profiles in the PanINs of either *Smad4* genotype; strong staining was noted for vimentin and PDGFRβ, while SMA was absent in the earliest PanINs—except in the perivascular smooth muscle cells—indicating the apparent absence of stellate cell activation in these incipient lesions, whereas established PanINs showed induction of SMA regardless of *Smad4* status (Fig. 5E; Supplementary Fig. 3A). Analysis of inflammatory cells revealed increases in macrophages in the *Smad4* mutant lesions although these differences did not reach statistical significance (Supplementary Fig. 3B). Overall, these results indicate that *Smad4* deficiency is associated with increased proliferation of both the neoplastic epithelium as well as the stromal tissue. This may suggest that Smad4 has both cell-autonomous and non-cell-autonomous functions in the pancreas, whereas alternatively, the stromal alterations may be secondary to epithelial proliferation. Finally, E-cadherin—a strongly induced protein in human PanIN—was also elevated in the murine lesions with notable increased staining intensity in the *Smad4*-deficient PanIN and metaplastic epithelium, suggesting Smad4-depedent alterations in the epithelial program (Fig. 5E; see below).

Smad4-deficiency promotes well-differentiated PDAC in the $Kras^{G12D}$ $Ink4a/Arf^{lox}$ model

Since the mice with combined $Kras^{G12D}$ expression and *Smad4* deletion showed rapid onset of IPMN and advanced PanIN lesions but exhibited only moderate malignant progression of pancreatic tumors, and since *SMAD4* loss occurs with concurrent *INK4A* loss and *KRAS* activation in human PDAC, we assessed subsequently the combined impact of *Smad4* and *Ink4a/Arf* mutations in *Cre LSL-$Kras^{G12D}$* mouse PanIN/PDAC models. Similar to our previous report (Bardeesy et al. 2006), $Kras^{G12D}$ and *Ink4a/Arf* heterozygosity cooperated to promote PDAC progression in *Cre LSL-$Kras^{G12D}$ $Ink4a/Arf^{lox/+}$* mice. A pronounced cooperative effect of *Smad4* deletion was noted with *Ptf1a-Cre LSL-$Kras^{G12D}$ $Smad4^{lox/lox}$ $Ink4a/Arf^{lox/+}$* mice showing significantly reduced survival relative to *Cre LSL-$Kras^{G12D}$ Ink4a/$Arf^{lox/+}$* controls (mean survival 14.0 wk vs. 38.0 wk; $p < 0.001$) (Fig. 6A). This reduced survival was associated with PDAC in 12/13 mice, IPMN in 1/13 mice, and concomitant IPMN and PDAC in four out of 13 animals (Fig. 6B; see Table 1). *Pdx1-Cre LSL-$Kras^{G12D}$ $Smad4^{lox/lox}$ $Ink4a/Arf^{lox/+}$* mice also showed a shortened survival (mean 12.6 wk) associated with PDAC in four out of 12 mice, gastric cancer in eight out of 12 mice (including one with PDAC and four with IPMN) (see Table 1). Six out of 16 *Smad4*-deficient PDACs showed liver metastasis or invasion (Supplementary Fig. 1C).

Western blot analysis of early passage PDAC cell lines revealed absence of Smad4 expression in all tumors from the $Smad4^{lox/lox}$ mice and retention of expression in all PDACs from $Smad4^{+/+}$ animals (Fig. 6C). Absence of $p16^{Ink4a}$ and $p19^{Arf}$ expression was documented in each of these tumor cell lines, regardless of germline *Smad4* status, and was associated with loss of the wild-type *Ink4a/Arf* allele (Fig. 6C; data not shown). p53 was intact in all cases as determined by $p21^{CIP}$ induction following exposure of the cell lines to ionizing radiation (data not shown). These genetic studies and molecular profiles show that *Smad4* deficiency promotes the development of IPMN in $Kras^{G12D}$ mutant mice independently of *Ink4a/Arf* mutation, while *Ink4a/Arf* mutations are required for full malignant progression to PDAC in the context of $Kras^{G12D}$ and *Smad4* inactivation.

Smad4 deficiency also altered the tumor phenotypes of mice with combined $Kras^{G12D}$ activation and homozygous *Ink4a/Arf* deletion; *Pdx1-Cre LSL-$Kras^{G12D}$ $Smad4^{lox/lox}$ $Ink4a/Arf^{lox/lox}$* mice ($n = 10$) had a slightly decreased survival (7.4 wk vs. 8.6 wk in *Pdx1-Cre LSL-$Kras^{G12D}$ $Ink4a/Arf^{lox/lox}$* mice; $p = 0.01$) with nine out of 10 mice displaying PDAC, five out of 10 mice harboring gastric cancers, and three out of 10 with IPMN coincident with the other tumors (Table 1). *Ptf1-Cre LSL-*

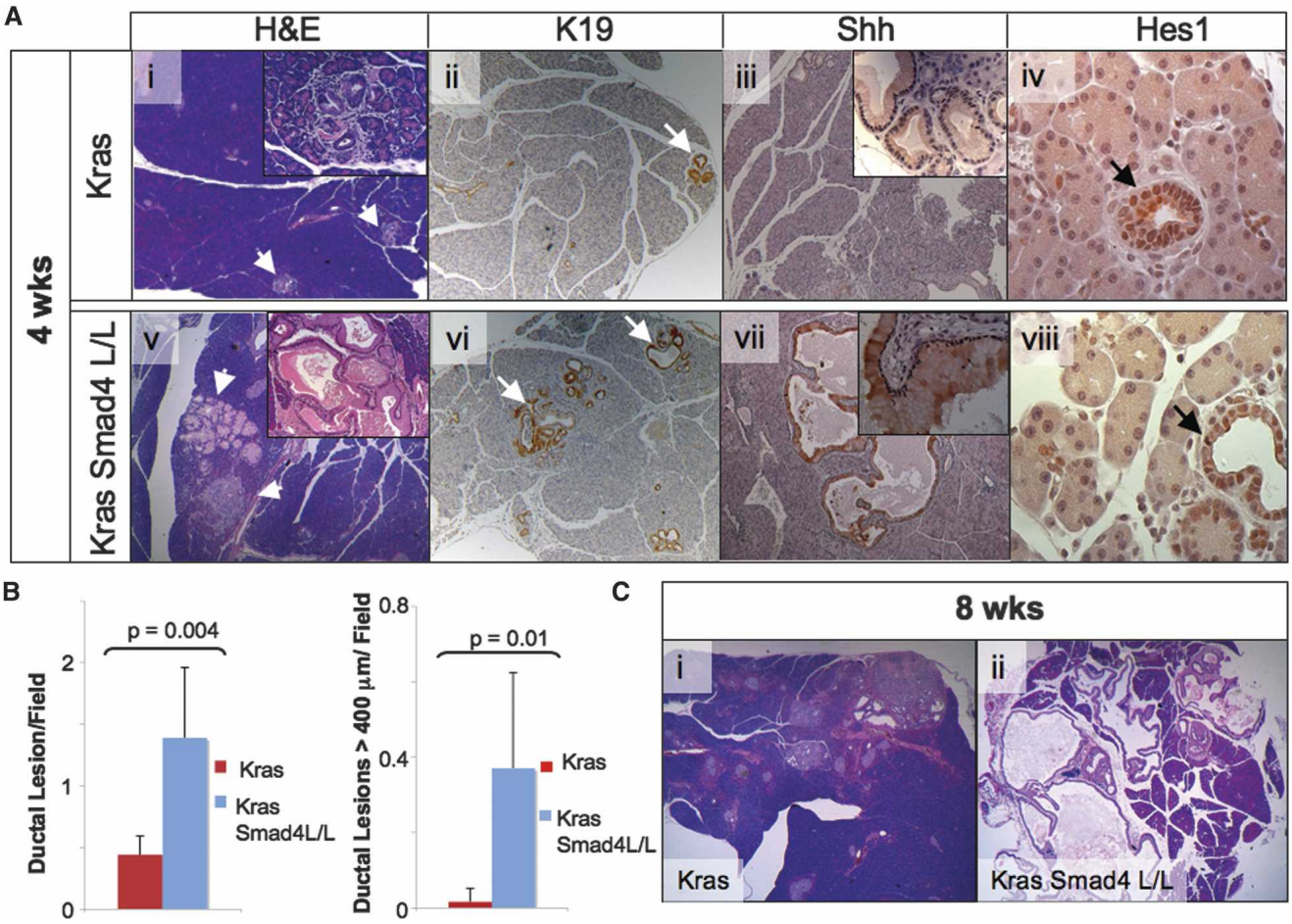

Figure 4. Comparison of evolving pancreatic lesions in *LSL-Kras*^{G12D} mice with intact or deleted *Smad4* alleles. (*A*) Pancreas specimens from 4-wk-old *Ptf1-Cre LSL-Kras*^{G12D} (panels *i–iv*) and *Ptf1-Cre LSL-Kras*^{G12D} *Smad4*$^{lox/lox}$ (panels *v–vii*) mice were stained with H&E (panels *i,v*) and with antibodies to cytokeratin-19 (panels *ii,vi*), Sonic Hedgehog (panels *iii,vii*) and Hes1 (panels *iv,viii*). The arrows point to pancreatic ductal lesions. (*B*) Morphometric analysis of pancreata from 4- to 5-wk-old *Ptf1-Cre LSL-Kras*^{G12D} and *Ptf1-Cre LSL-Kras*^{G12D} *Smad4*$^{lox/lox}$ mice (see Materials and Methods). (*Left* panel) Graph of number of ductal lesions per 100× field. (*Right* panel) Graph of number of ductal lesions per 100× field measuring >400 µm at greatest diameter. Six mice per genotype were analyzed with a minimum of eight fields counted per mouse. (*C*) H&E-stained pancreas from 8-wk-old *Ptf1-Cre LSL-Kras*^{G12D} (panel *i*) and *Ptf1-Cre LSL-Kras*^{G12D} *Smad4*$^{lox/lox}$ (panel *ii*) mice. Magnifications: *A* (panels *i–iii,v–vii*), *C* (panels *i,ii*), 50×; *A* (*insets* in panels *i,v*), 200×; *A* (*insets* in panels *iii,vii*), 400×.

Kras^{G12D} *Smad4*$^{lox/lox}$ *Ink4a/Arf*$^{lox/lox}$ mice (four of four) developed PDAC with a mean latency of 8.8 wk, indicating that *Smad4* status did not accelerate PDAC in context of homozygous *Ink4a/Arf* deletion.

Next, as human and mouse PDACs are known to present with a range of distinct histopathological phenotypes—from well-differentiated, wherein tumor cells form discernable duct-like/glandular structures, to undifferentiated carcinomas that may arise from EMT of the glandular epithelium (Solcia et al. 1995; Hruban et al. 2006)—and Smad4/TGF-β signaling has been implicated in processes of epithelial differentiation (for review, see Zavadil and Bottinger 2005), we sought to determine whether *Smad4* status influenced the morphological presentation of the *Cre LSL-Kras*^{G12D} *Ink4a/Arf* mutant models. Upon placement on the *Smad4*-deficient background, there was a significant decrease in the proportion of undifferentiated carcinomas in *Cre Kras*^{G12D} *Ink4a/Arf* $^{lox/lox}$ and *Cre Kras*^{G12D} *Ink4a/Arf* $^{lox/+}$ mice: from 26.7% and 43% to 7.7% and 12.5%, respectively (Table 2). The *Smad4*-deficient PDACs typically showed well-to-moderately-differentiated (ductal) histology and strong cytokeratin-19 staining in contrast to the weak signal detected in regions of undifferentiated histology frequently noted in the *Smad4*$^{+/+}$ tumors (Fig. 6D, cf. panels i,ii and v,vi; note transition between undifferentiated and ductal histology in panel ii). These observations suggest that active TGF-β/Smad4 signaling may contribute the loss of epithelial differentiation in PDAC, as observed in skin and breast cancers (for review, see Bierie and Moses 2006).

TGF-β-mediated induction of the Snail and Slug transcriptional repressors and consequent repression of E-cadherin expression contribute to EMT in several cell

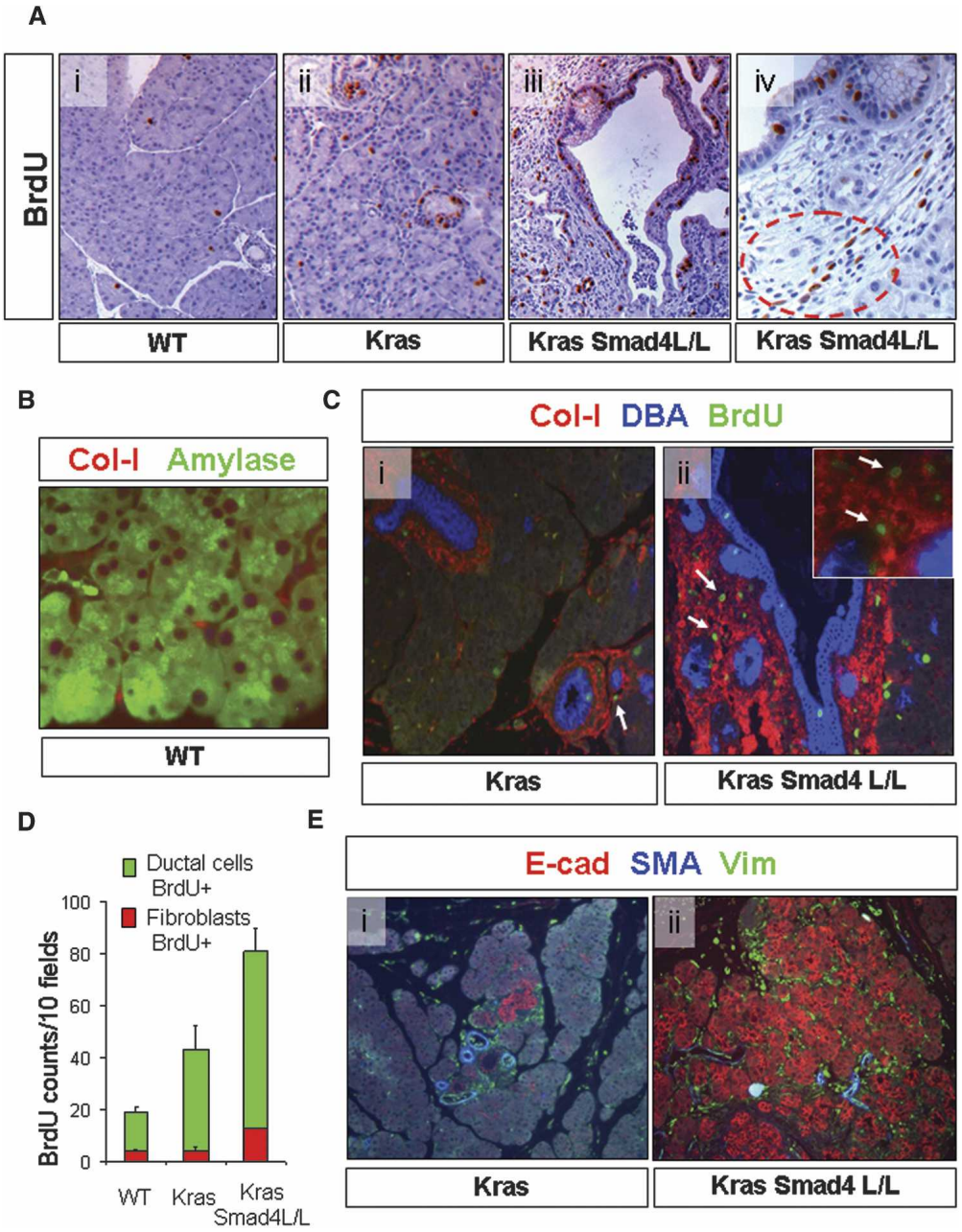

Figure 5. *Smad4* deficiency cooperates with $Kras^{G12D}$ to promote epithelial and stromal expansion. (*A*) BrdU labeling of pancreata from wild-type (panel *i*), *Ptf1-Cre LSL-*$Kras^{G12D}$ (panel *ii*), and *Ptf1-Cre LSL-*$Kras^{G12D}$ $Smad4^{lox/lox}$ (panel *iii*) mice. (Panel *iv*) High-power view of proliferating epithelial and stromal cells (circled) in evolving PanIN from *Ptf1-Cre LSL-*$Kras^{G12D}$ $Smad4^{lox/lox}$ mice. (*B*) Immunofluorescence staining of wild-type mouse pancreas with antibodies against amylase (green) and collagen-1 (red) demonstrating the periacinar location of pancreatic fibroblasts. (*C*) Staining of ductal lesions from *Ptf1-Cre LSL-*$Kras^{G12D}$ (panel *i*) and *Ptf1-Cre LSL-*$Kras^{G12D}$ $Smad4^{lox/lox}$ (panel *ii*) mice with DBA lectin (blue) and with antibodies to collagen-1 (red) and BrdU (green) reveals proliferation in both the PanIN epithelium and fibroblastic components. (Panel *ii*) *Inset* is a high-power view showing fibroblast proliferation (arrows). (*D*) Graph of number of BrDU-positive epithelial and fibroblast cells per 200× field; three mice per genotype were analyzed. (*E*) Immunofluorescence staining of pancreata from 4-wk-old *Ptf1-Cre LSL-*$Kras^{G12D}$ (panel *i*) and *Ptf1-Cre LSL-*$Kras^{G12D}$ $Smad4^{lox/lox}$ (panel *ii*) mice with antibodies to E-cadherin (red), smooth muscle actin (blue), and vimentin (green). Magnifications: *H* (panels *i*,*ii*), 50×; *A–C*,*F* (panels *i*,*ii*), 100×; *C*, *inset*, 200×; *D*,*E*, 400×.

types (for review, see Zavadil and Bottinger 2005). Correspondingly, PDACs from $Smad4^{+/+}$ mice showed frequent loss of E-cadherin and elevation of Slug expression compared with PDACs from $Smad4^{lox/lox}$ mice as demonstrated by immunostaining of primary tumors (Fig. 6D) and Western blot analyses of PDAC cell lines (Fig. 7A). The sustained high level of E-cadherin in the *Smad4* mutant tumors was confirmed by qRT–PCR analysis

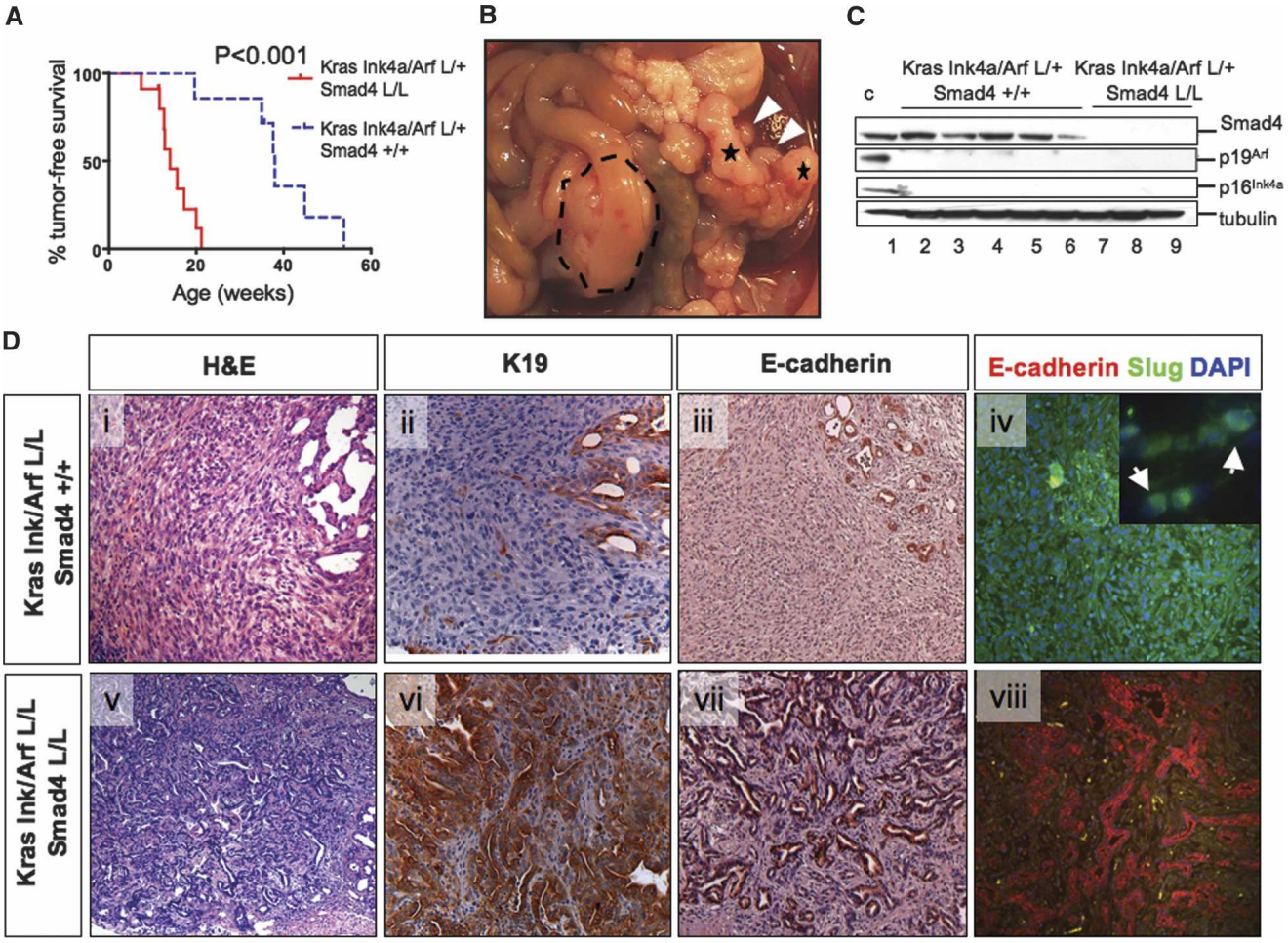

Figure 6. *Smad4* deletion promotes the glandular PDAC in cooperation with $Kras^{G12D}$ activation and *Ink4a/Arf* deficiency. (*A*) Kaplan-Meier analysis showing pancreas tumor-free survival of *Ptf1a-Cre LSL-*$Kras^{G12D}$ *Ink4a/*$Arf^{lox/+}$ **$Smad4^{lox/lox}$ mice and *Ptf1a-Cre LSL-*$Kras^{G12D}$ *Ink4a/*$Arf^{lox/+}$ *Smad4*$^{+/+}$ mice. Twelve of 13 deaths in the *Ptf1a-Cre LSL-*$Kras^{G12D}$ *Ink4a/*$Arf^{lox/+}$ *Smad4*$^{lox/lox}$ mice were due to PDAC, and one out of 13 was due to IPMN. (*B*) PDAC arising in a *Ptf1a-Cre LSL-*$Kras^{G12D}$ *Ink4a/*$Arf^{lox/+}$ *Smad4*$^{lox/lox}$ mouse (indicated by dashed line); note the liver metastases (white arrowheads). This mouse also showed an IPMN (denoted by asterisks). (*C*) Western blot analysis of lysates from early passage PDAC cell lines from the *Ptf1a-Cre LSL-*$Kras^{G12D}$ *Ink4a/*$Arf^{lox/+}$ *Smad4*$^{+/+}$ (lanes *2–6*) and *Ptf1a-Cre LSL-*$Kras^{G12D}$ *Ink4a/*$Arf^{lox/+}$ *Smad4*$^{lox/lox}$ (lanes *7–9*) models for expression of Smad4, $p19^{Arf}$, $p16^{Ink4a}$, and tubulin. Lane *1* shows positive controls. (*D*) Undifferentiated PDAC from a *Ptf1a-Cre LSL-*$Kras^{G12D}$ *Ink4a/*$Arf^{lox/+}$ mouse (panels *i–iv*) and a moderately differentiated PDAC from a *Ptf1a-Cre LSL-*$Kras^{G12D}$ *Ink4a/*$Arf^{lox/+}$ *Smad4*$^{lox/lox}$ mouse (panels *v–viii*) stained with H&E (panels *i*,*v*), or with antibodies to cytokeratin-19 (panels *ii*,*vi*) and E-cadherin (panel *iii*,*vii*), and double-labeled with antibodies to E-cadherin (red) and Slug (green) (panels *iv*,*viii*). Magnifications: All are 100× except *D* (panel *iv*, *inset*), which is 630×.

(Fig. 7B). The S100A4/FSP1 protein has been shown to promote EMT in cancer cell lines while also marking a subset of fibroblasts (Okada et al. 1997). The PDAC stromal fibroblasts showed strong S100A4 staining regardless of *Smad4* status; on the other hand, while the tumor cells in the *Smad4*$^{+/+}$ tumors frequently stained positive for S100A4, staining was uncommon in the *Smad4*-deficient tumor epithelium (Fig. 7C). Overall, these results are consistent with a role of TGF-β–Smad4 signaling in controlling the PDAC cellular differentiation phenotype, possibly through regulation of Slug expression.

In addition, to the differences in tumor cell morphology, the *Smad4* mutant tumors exhibited differences in stromal fibroblast content, as readily observed in histological sections. This increased fibrosis was confirmed by Western blot and IHC for collagen-1 expression (Supplementary Fig. 4A,B). There also appeared to be a trend toward an increased number of inflammatory cells

Table 2. *Impact of Smad4 status on PDAC histology*

Genotype[a]	Percent sarcomatoid histology
KrasG12D Ink4a/Arf L/L	8/30 (26.7%)
KrasG12D Ink4a/Arf L/L Smad L/L	1/13 (7.7%)
KrasG12D Ink4a/Arf L/+	6/14 (43%)
KrasG12D Ink4a/Arf L/+ Smad L/L	2/16 (12.5%)

[a]All mice have either the Pdx1-Cre or Ptf1a-Cre alleles.

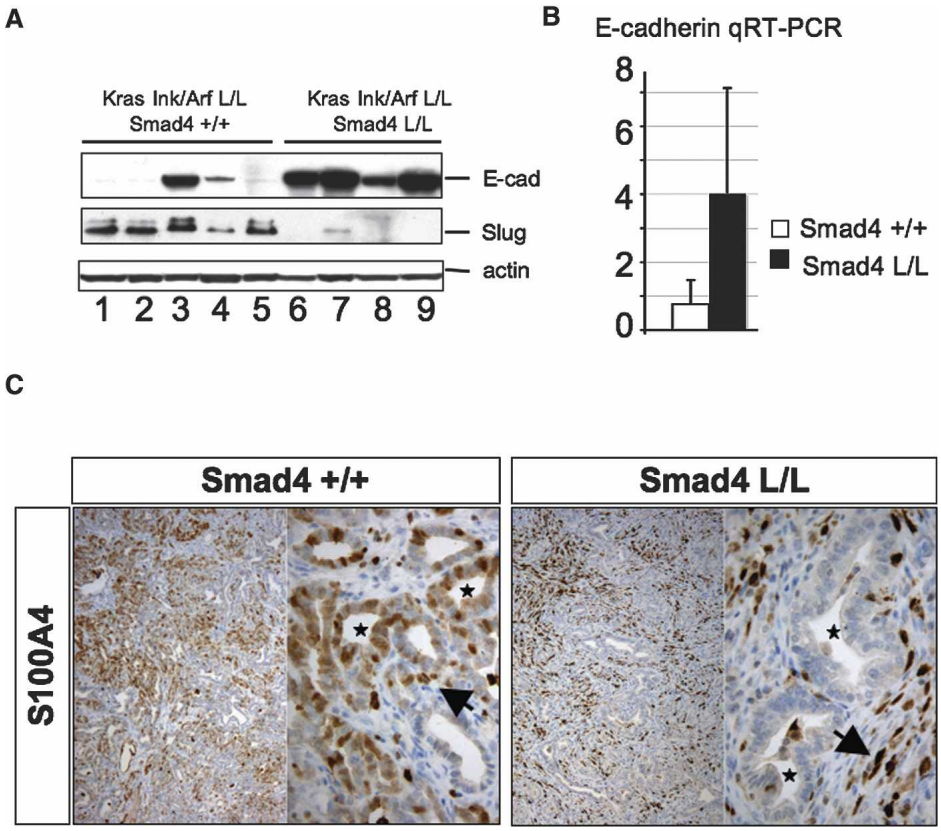

Figure 7. Retention of epithelial differentiation in *Smad4*-deficient PDAC. (*A*) Western blot showing E-cadherin (*top* panel) and slug expression (*middle* panel) in PDAC cell lines from *Cre LSL-Kras^{G12D} Ink4a/Arf$^{lox/lox}$ Smad4$^{+/+}$* mice (lanes *1–5*) and *Cre LSL-Kras^{G12D} Ink4a/Arf$^{lox/lox}$ Smad4$^{lox/lox}$* (lanes *6–9*) mice. (*B*) qRT–PCR for E-cadherin expression in primary PDAC from *Cre LSL-Kras^{G12D} Ink4a/Arf$^{lox/+}$ Smad4$^{+/+}$* mice and *Cre LSL-Kras^{G12D} Ink4a/Arf$^{lox/+}$ Smad4$^{lox/lox}$* mice. (*C*) IHC analysis of S100A4 expression in PDAC from a *Ptf1-Cre LSL-Kras^{G12D} Ink4a/Arf$^{lox/+}$ Smad4$^{+/+}$* mouse and a *Ptf1-Cre LSL-Kras^{G12D} Ink4a/Arf$^{lox/+}$ Smad4$^{lox/lox}$* mouse; note the staining of stromal fibroblasts in both genotypes (arrows) and staining of tumor glands in the *Smad4$^{+/+}$* tumors but not those lacking *Smad4* (asterisks).

as assessed by staining for macrophages and neutrophils (Supplementary Table 1; data not shown). Finally, analysis of PDAC blood vessel density failed to reveal pronounced differences between genotypes when areas of similar histopathology were compared (Supplementary Fig. 4C; data not shown).

Smad4 modulates TGF-β sensitivity in murine PDAC cell lines

The genetically defined early passage PDAC cell lines described above, null and wild type for *Smad4*, provided an opportunity to understand better the cell biological impact of TGF-β–Smad4 signaling in this system. PDAC cell lines from *Smad4$^{lox/lox}$* mice ($n = 4$ cell lines) were completely resistant to TGF-β-induced growth inhibition (see below), whereas those from the *Smad4$^{+/+}$* models showed differential sensitivity; *Smad4$^{+/+}$* cell lines derived from well or moderately differentiated (ductal) tumors exhibited growth inhibition and cell death ($n = 4$ cell lines), whereas those from undifferentiated tumors showed increased proliferation ($n = 3$ cell lines) (Fig. 8A; Table 3). Similar profiles were observed in scratch assays; ductal *Smad4$^{+/+}$* cell lines showed decreased migration upon TGF-β exposure, while enhanced migration was seen in the undifferentiated *Smad4$^{+/+}$* lines (Fig. 8B; Table 3). The *Smad4*-deficient lines also showed a modest increase in migration in response to TGF-β.

Next, we assessed whether restoration of *Smad4* in *Smad4*-deficient PDAC cell lines affected TGF-β responsiveness. Retroviral-mediated expression of *Smad4*, but not GFP, in the *Smad4*-deficient lines ($n = 3$ cell lines) restored TGF-β-induced growth inhibition but had no effect on basal proliferation in the absence of exogenous TGF-β treatment (Fig. 9A,B; Table 3). In the presence of TGF-β treatment, the *Smad4*-reconstituted and wild-type cell lines (specifically those with a ductal phenotype) lost both their epithelial morphology and E-cadherin staining at the cell junctions before undergoing cell death, whereas no cytological changes were observed in GFP-transduced *Smad4*-deficient cultures (Fig. 9C,D). Overall, these results are consistent with the view that *Smad4* inactivation facilitates PDAC progression by disabling TGF-β-mediated cytotoxicity while indicating that TGF-β acts to promote growth of a subset of PDAC with *Smad4* intact and with an undifferentiated cellular phenotype.

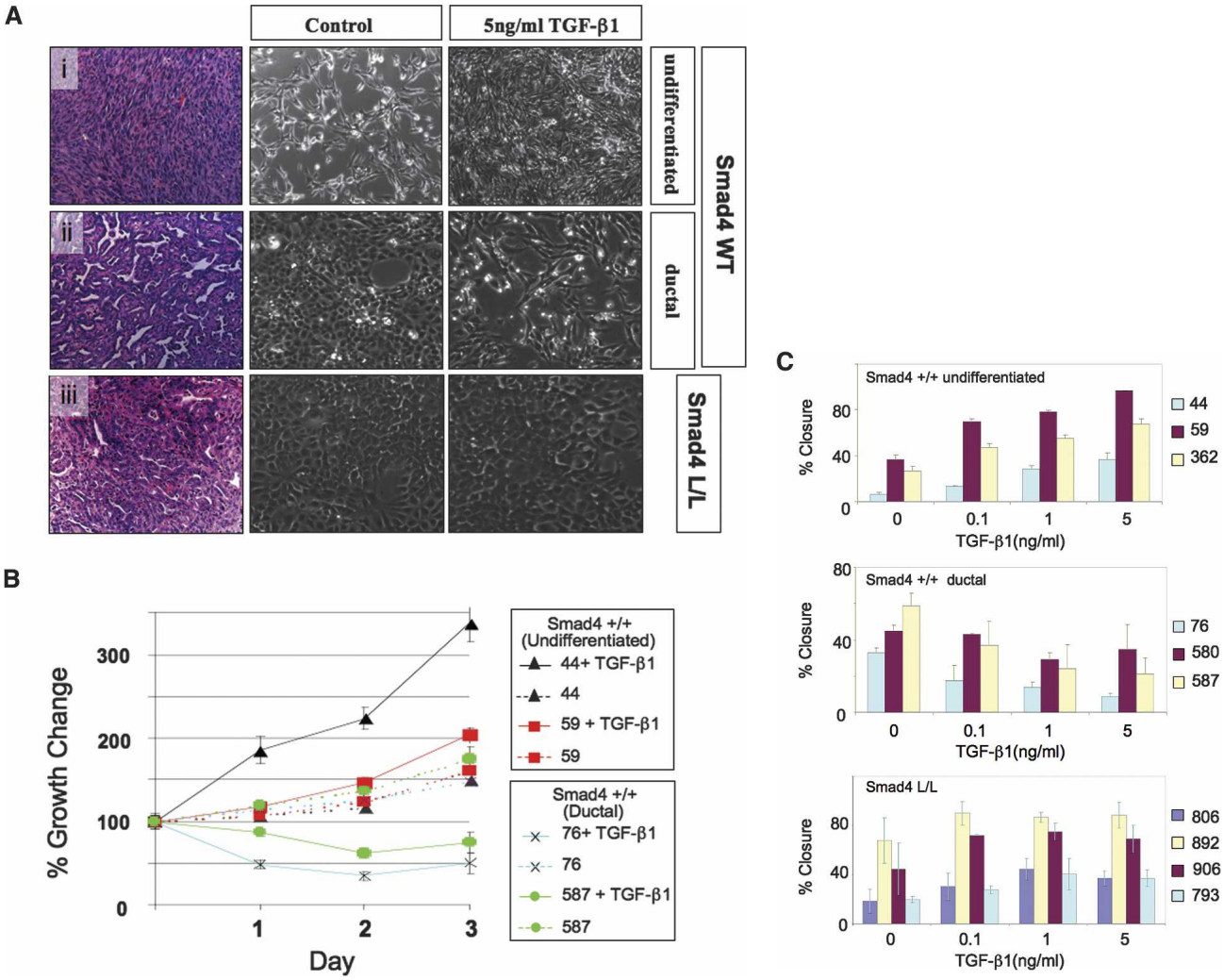

Figure 8. Smad4 status modulates TGF-β responses in PDAC. (*A*) H&E-stained sections showing PDAC histology (*left* panels), and images of derivative cell lines either mock-treated (center) or exposed to 5 µg/mL TGF-β (*right* panels) from *Smad4* wild-type undifferentiated tumors (panel *i*), *Smad4* wild-type ductal tumors (panel *ii*), and *Smad4*-null tumors (panel *iii*). Note that TGF-β enhances growth in panel *i* and inhibits in panel *ii* while no effect is seen in panel *iii*. Magnifications, 100×. (*B*) Growth curves of Smad4$^{+/+}$ PDAC cell lines in 0.5% serum in the presence or absence of 5 µg/mL TGF-β. (*C*) Graphs of scratch assay measuring cell migration as relative wound closure after 16 h in the presence or absence of TGF-β1.

Discussion

In this study, we have shown that *Smad4* is dispensable for normal pancreas development and physiology and functions to constrain progression of Kras^{G12D}-initiated neoplasms with a corresponding impact on the biology of tumor cells and their microenvironment. *Smad4* deficiency led to rapid progression of pancreatic tumors in the context of activated *Kras*^{G12D}, alone or in combination with *Ink4a/Arf* mutation, and was able to shift *Kras*^{G12D}-initiated neoplasms toward an alternative histological pathway to advanced PDAC, one that is characterized by an IPMN presentation observed in some human cases. Along similar lines, *Smad4* deficiency also influenced the differentiation state of *Kras*^{G12D} *Ink4a/Arf* mutant PDACs, producing tumors that retained epithelial differentiation in contrast to the frequent EMT observed in pancreatic cancers with intact *Smad4*. This system affords an opportunity to systematically understand the role of the TGFβ–SMAD axis in many complex aspects of tumorigenesis including tumor cell proliferation, migration, survival, and differentiation as well as the tumor microenvironment including angiogenesis. As such, this genetic model provides a framework for understanding how to deploy agents targeting this pathway in human PDAC.

Impact of SMAD4 on pancreas development and physiology

The normal pancreatic development and function in the *Pdx1-Cre Smad4*$^{lox/lox}$ mice was not anticipated and contrasts with diverse pancreatic phenotypes associated

Table 3. *TGF-TGF-β1 responsiveness of PDAC cell lines*

Genotype	Phenotype	Name	Response to TGF-β1	
			Proliferation	Migration
Smad4$^{+/+}$	Ductal	65	Decreased	Decreased
		76	Decreased	Decreased
		580	Decreased	—
		587	Decreased	Decreased
		743	Decreased	N.D.
	Undifferentiated	44	Increased	Increased
		59	Increased	Increased
		362	Increased	Increased
Smad4$^{-/-}$	Ductal	806	—	—
		806 + Smad4	Decreased	N.D.
		792	—	—
		792 + Smad4	Decreased	N.D.
		892	—	—
		892 + Smad4	Decreased	N.D.
		874	—	—

(—) No significant effect; (N.D.) not done.

with other experimental perturbations of TGF-β family signaling. For example, acinar-to-ductal metaplasia or autoimmune pancreatitis is observed in different transgenic models expressing a dominant-negative *TGF-βRII* mutant in the pancreatic acinar cells (Bottinger et al. 1997; Hahm et al. 2000). Null mutations in the Activin signaling pathway are associated with gross pancreatic defects (Kim et al. 2000; Harmon et al. 2004). Overexpression of the inhibitory *Smad*, *Smad7*, results in pancreatic malformations and β-islet cell defects (Smart et al. 2006). Finally, expression of a dominant-negative Smad4 mutant in the acinar cells results in an age-dependent increase in islet size (Simeone et al. 2006). These phenotypes, coupled with normal pancreas development and function in the *Pdx1-Cre Smad4$^{lox/lox}$* mice, suggest roles for Smad4-independent TGF-β signaling pathways in these processes (Bierie and Moses 2006) and/or point to nonphysiological gain-of-function activities of ectopically overexpressed proteins. The dispensability of *Smad4* for pancreatic organogenesis mirrors what has been observed in the liver and breast (Li et al. 2003; Wang et al. 2005); in contrast, Smad4 is required during early development to pattern derivatives of the anterior primitive streak and for formation of extraembryonic lineages (Chu et al. 2004). Overall, genetic studies have consistently revealed a more prominent role for *Smad4* mediating TGF-β-regulated developmental processes relating to early specification and patterning rather than cytodifferentiation during later stages of organogenesis.

Kras^{G12D} expression and Smad4 inactivation results in pancreatic ductal tumorigenesis

Our study demonstrates strong genetic interaction between *Kras^{G12D}* and *Smad4* in the development of IPMN and PDAC. IPMN is being increasingly recognized as an important clinical condition due to its propensity to progress to lethal PDAC (Maitra et al. 2005). Unlike PanIN, IPMN has recognizable clinical signs and can be detected noninvasively in the absence of malignant disease. Hence, improved understanding of the biology of these lesions could inform the design of treatments that prevent the onset of PDAC. While *SMAD4* inactivation is associated with progression to advanced histological stages in human IPMN, our data indicate that *SMAD4* can also act to restrain the initiation of these neoplasms. While *Ink4a/Arf* loss has been implicated in other cystic pancreatic tumors (Bardeesy et al. 2002a), it did not contribute to these IPMNs. Homozygous *Smad4* deletion also cooperatively induced rapid PDAC progression, particularly in the context of *Kras^{G12D}* and *Ink4a/Arf* heterozygosity. Together, these results indicate that *Smad4* and the *Ink4a/Arf* locus regulate distinct pathways that contribute to PDAC tumor suppression, with *Ink4a/Arf* playing a more critical role in restricting malignant progression.

A related study has investigated the impact of inactivation of the *Tgf-βRII* on pancreatic tumorigenesis (H. Ijichi and H.L. Moses, pers. comm.). This study showed that *Ptf1-Cre LSL-Kras^{G12D} Tgf-βRII$^{lox/lox}$* mice develop PDAC by 10 wk of age without exhibiting IPMN. The more rapid PDAC progression in this model compared with our *Smad4*-deficient model is likely to reflect a role for Smad4-independent pathways downstream from *Tgf-βRII* (Bierie and Moses 2006), although differences in genetic background cannot be ruled out. Likewise, the absence of IPMN in the *Tgf-βRII*-deficient mice may relate to the role of Smad4 in mediating signals from other classes of TGF-β family receptors; notably, BMPs and Activins are also induced in evolving PDAC, and inactivation of their receptors is associated with gastrointestinal malignancy (Howe et al. 2001; Jung et al. 2004). Hence, the IPMN phenotype may involve defects in a combination of these pathways. The detailed molecular

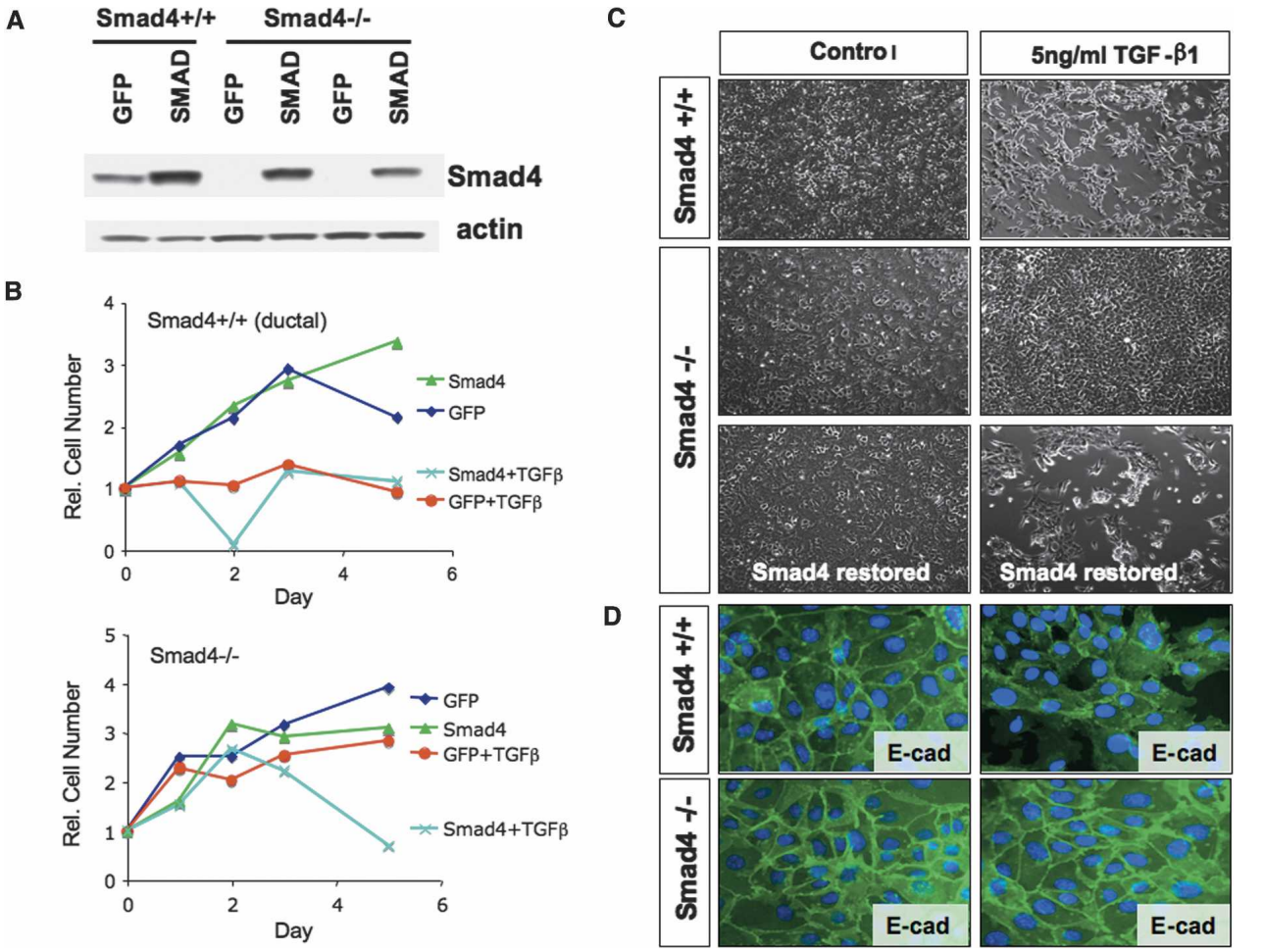

Figure 9. Smad4 expression restores TGF-β-responsiveness in *Smad4*-deficient PDAC cell lines. (*A*) Western blot analysis for Smad4 expression in PDAC cell lines from *Pdx1-Cre LSL-Kras*^{G12D} *Ink4a/Arf*$^{lox/+}$ and *Pdx1-Cre LSL-Kras*^{G12D} *Ink4a/Arf*$^{lox/+}$ *Smad4*$^{lox/lox}$ mice that were transduced with retroviruses expressing *Smad4* or *GFP*. (*B*) Growth curves of the transduced PDAC cell lines in the presence or absence of TGF-β. (*C*) Morphology of PDAC cells with or without TGF-β treatment. The cells were photographed after 5 d of treatment with TGF-β or vehicle. (*D*) Impact of TGF-β administration on E-cadherin localization. E-cadherin staining is lost at the cellular junctions following TGF-β treatment in PDAC cell lines with intact *Smad4* but not in cell lines with *Smad4* inactivation.

comparison of these models may provide valuable insights into nonoverlapping PDAC tumor suppressor pathways that are differentially regulated by *Smad4* and *Tgf-βRII*. Overall, given the more potent impact of *Tgf-βRII* inactivation on *Pdx1-Cre LSL-Kras*^{G12D}-driven PDAC development compared with that of *Smad4* inactivation, it is curious that PDACs in humans show exclusively *Smad4* mutations, while *Tgf-βRII* mutations are restricted to a medullary pancreatic cancer, a rare variant associated with mismatch repair defects (Venkatasubbarao et al. 1998; Wilentz et al. 2000).

Smad4 regulates EMT in PDAC

Our demonstration that *Smad4* deficiency promoted progression to PDAC but produced tumors that retained differentiated ductal histopathology is consistent with a bimodal role of TGF-β–Smad4 signaling in regulating the biology of this cancer. Our studies showed that, consistent with well/moderately differentiated histology, *Smad4*-deficient invasive tumors retained E-cadherin expression and were far less likely than *Smad4* wild-type tumors to show S100A4 expression, a calcium-binding protein implicated in cell motility, EMT, and metastases (Okada et al. 1997; Helfman et al. 2005) that has been associated with poor differentiation and prognosis in PDAC (Rosty et al. 2002). In addition, in vitro studies with our early passage PDAC revealed that while *Smad4* deficiency was associated with attenuated TGF-β responsiveness, Smad4-expressing lines showed two classes of prominent responses: increased proliferation and migration of undifferentiated Smad4$^{+/+}$ lines and cell death in well-differentiated lines.

Although an association between *SMAD4* status and tumor cell differentiation in human PDAC has not been clearly established, SMAD4 expression tracked with

poor cellular differentiation in a morphometric study of human PDAC cell lines; poor differentiation was observed in four out of six *SMAD4* wild-type versus zero out of five *SMAD4* mutant lines (Sipos et al. 2003). Furthermore, in studies of a series of 16 human PDAC cell lines grown as xenografts, we observed that undifferentiated histology was only in tumors derived from *SMAD4* wild-type cell lines, although one undifferentiated line had TGFβRII defects (data not shown). Our data suggest that *Smad4* status and tumor cell differentiation may be important in determining which subset of PDAC depends on active TGF-β signaling for ongoing tumorigenic growth. An implication of our work is that *Smad4* status could potentially predict which set of tumors is likely to respond to TGF-β inhibition, although further studies will be needed to validate this hypothesis.

Materials and methods

Generation of a conditional Smad4 mouse strain

A BAC clone containing the *Smad4* locus was identified by screening a 129SV/ev library (Children's Hospital of Oakland). The targeting construct was generated in the pKOII vector (Bardeesy et al. 2002b) and consisted of an 8.6-kb EcoRV–MscI fragment (long arm) containing *Smad4* exons 7–9 and a 2.1-kb MscI–EcoRV fragment (short arm). A *loxP* site was inserted at a StuI site flanking *Smad4* exons 8 and 9 (see Fig. 1A) enabling Cre-mediated deletion of a 1.4-kb fragment containing exons 8 and 9. Gene targeting in 129SV/ev embryonic stem (ES) cells and generation of chimeric animals were performed using standard techniques. The *Frt*-flanked *PGK-neo* cassette was excised by crosses to *Actin-Flpe* mice (Rodriguez et al. 2000), generating the $Smad4^{Lox}$ allele. Mice were backcrossed ($N = 5$) on an FVB/n background, eliminating the *Actin-Flpe* allele.

Mouse strains, histopathology, and establishment of primary PDAC cell lines

In addition to the $Smad4^{Lox}$ mice, the mouse strains in this study included the following alleles: $LSL\text{-}Kras^{G12D}$ (Aguirre et al. 2003), *Pdx1-Cre* (Gu et al. 2002), *Ptf1a-Cre* (Kawaguchi et al. 2002), and $p16^{Ink4a}/p19^{Arflox}$ (Aguirre et al. 2003; Bardeesy et al. 2006). All experiments were performed on >96.9% FVB/n background. Tissue processing, immunohistochemical staining, and establishment of primary PDAC cell lines were performed as described (Aguirre et al. 2003). For frozen sections, tissues were immediately embedded in OCT (Sakura Finetek) and frozen on dry ice. Fixation, blocking, and antibody incubation were by standard procedures. Coverslips were mounted on fluorescently labeled tissue using Vectamount with DAPI (Vector Laboratories). Images were captured using a Leica DM1400B microsystem and Leica FW4000 version 1.2.1.

Antibodies

The antibodies used for immunoblot analyses were $p16^{Ink4a}$ (M-156), Smad4 (B-8) and p21 (C-19) (Santa Cruz Biotechnology), $p19^{Arf}$ (Ab-80, Abcam), tubulin (DM-1A) and Actin (Sigma), Slug (Abgent), E-cadherin (Invitrogen), and phospho Smad2 (Chemicon International). The antibodies for immunohistochemical analysis were amylase (Sigma); rat monoclonal cytokeratin-19 (TROMA3; kindly provided by Dr. R. Kemler, Max Planck Institute, Freiburg, Germany); E-cadherin (Zymed; Invitrogen); Glucagon (Dako); Insulin (Dako); Pdx-1 (a kind gift of Dr. C. Wright, Vanderbilt University, Nashville, TN); TGFβ1, BMP4, Muc2, Shh, Vimentin, and PDGFR-β (Santa Cruz Biotechnology); Smad2/3 and BrdU (BD; Transduction Laboratories); Muc5AC (Labvision); Muc1 (CT2 monoclonal antibody; a kind gift of Dr. S. Gendler, Mayo Clinic, Scottsdale, AZ); Muc4 (Dr. K. Carraway, University of Miami, Miami, FL); CDX2 (Biogenex); Hes1 (a kind gift of Dr. T. Sudo, Toray Scientific, Kanagawa, Japan); Collagen type I (Abcam); SMA (Novus); phospho-Stat3 (Ser727); and phospho-p44/42 (T202/Y204) and phospho-Akt (Ser473) (Cell Signaling). The following antibodies were used on frozen sections: rabbit MMP-9 (a kind gift from Dr. Z. Werb, University of California at San Francisco, San Francisco, CA); monoclonal rat anti-Meca-32 (Pharmingen); F4/80 (Serotec); PMN antibody (clone 7/4; Cedarlane Laboratories); PDGFRβ and PDGFRα monoclonal antibodies (eBioscience); and rabbit CSF1R (Upstate Biotechnology/Chemicon).

Molecular and cellular analyses

RNA and DNA isolation, protein extract preparation from PDAC cell lines and primary tumors, and Western blots were performed as described (Aguirre et al. 2003). For cell proliferation assays, cells were seeded on 96-well plates at a density of 2×10^3 to 4×10^3 per well in 100 µL of culture media with 0.5% FBS. The media were replaced every other day. To evaluate cell proliferation, cells were incubated for 1–5 d with or without TGF-β1 treatment (R&D Systems) and assayed using the WST-1 Cell Proliferation Assay reagent (Roche). For cell migration analysis, in vitro wound healing assays were used to assess cell motility in two dimensions. Cells were plated on a six-well plate and grown to confluence in their regular medium. A 200-µL pipette tip was used to create a denuded area. Cells were washed twice with PBS and kept in RPMI medium containing 0.5% FBS in the presence or absence of TGF-β1 (5 ng/mL) for 16 h. Photographs were taken at hours 0, 10, and 16, and the distance traveled was determined by subtracting the values obtained at hour 0 from 16 h.

Statistical analysis

For morphometric studies of pancreatic lesions, a series of 36 consecutive 5-µm H&-stained sections was analyzed for each pancreas, and the sections with the greatest number of visible lesions were selected for quantitation; at least eight 100× fields were. For immunofluorescence, stained tissue was examined using a Zeiss Axioskop-2+ Microscope (fluorescently labeled tissues) with Openlab software (Improvision). F4/80, PMN, PDGFRβ, and MMP-9 expression was determined by counting the staining per field. Meca-32 staining was quantitated by counting the number of vessels per field. At least four fields were measured from each slide, and an average was calculated by nonpaired *t*-test analysis using InStat Software (GraphPad).

Acknowledgments

We thank David Tuveson and Tyler Jacks for the $LSL\text{-}Kras^{G12D}$ mice, Doug Melton for the *Pdx1-Cre* mice, and Chris Wright for the *Ptf1a-Cre* mice. We thank Dr. Kwok-kin Wong for critical reading of the manuscript. This work was support by grants NIH K01 CA104647 and NIH P01 CA117969-01, and grants from the Samuel Waxman Foundation and the Harvard Stem Cell Institute to N.B.; and grants P01 CA117969-01, 5U01CA84313-08, American Cancer Society Research Professorship, Ellison Medical Foundation, and the Robert A. and Renee E. Belfer Foundation Institute for Innovative Cancer Science to R.A.D.

References

Adsay, N.V., Merati, K., Basturk, O., Iacobuzio-Donahue, C., Levi, E., Cheng, J.D., Sarkar, F.H., Hruban, R.H., and Klimstra, D.S. 2004. Pathologically and biologically distinct types of epithelium in intraductal papillary mucinous neoplasms: Delineation of an 'intestinal' pathway of carcinogenesis in the pancreas. *Am. J. Surg. Pathol.* **28:** 839–848.

Aguirre, A.J., Bardeesy, N., Sinha, M., Lopez, L., Tuveson, D.A., Horner, J., Redston, M.S., and DePinho, R.A. 2003. Activated Kras and Ink4a/Arf deficiency cooperate to produce metastatic pancreatic ductal adenocarcinoma. *Genes & Dev.* **17:** 3112–3126.

Apte, M.V., Park, S., Phillips, P.A., Santucci, N., Goldstein, D., Kumar, R.K., Ramm, G.A., Buchler, M., Friess, H., McCarroll, J.A., et al. 2004. Desmoplastic reaction in pancreatic cancer: Role of pancreatic stellate cells. *Pancreas* **29:** 179–187.

Bardeesy, N., Morgan, J., Sinha, M., Signoretti, S., Srivastava, S., Loda, M., Merlino, G., and DePinho, R.A. 2002a. Obligate roles for p16(Ink4a) and p19(Arf)–p53 in the suppression of murine pancreatic neoplasia. *Mol. Cell. Biol.* **22:** 635–643.

Bardeesy, N., Sinha, M., Hezel, A.F., Signoretti, S., Hathaway, N.A., Sharpless, N.E., Loda, M., Carrasco, D.R., and DePinho, R.A. 2002b. Loss of the Lkb1 tumour suppressor provokes intestinal polyposis but resistance to transformation. *Nature* **419:** 162–167.

Bardeesy, N., Aguirre, A.J., Chu, G.C., Cheng, K.H., Lopez, L.V., Hezel, A.F., Feng, B., Brennan, C., Weissleder, R., Mahmood, U., et al. 2006. Both p16Ink4a and the p19Arf–p53 pathway constrain progression of pancreatic adenocarcinoma in the mouse. *Proc. Natl. Acad. Sci.* **103:** 5947–5952.

Biankin, A.V., Morey, A.L., Lee, C.S., Kench, J.G., Biankin, S.A., Hook, H.C., Head, D.R., Hugh, T.B., Sutherland, R.L., and Henshall, S.M. 2002. DPC4/Smad4 expression and outcome in pancreatic ductal adenocarcinoma. *J. Clin. Oncol.* **20:** 4531–4542.

Bierie, B. and Moses, H.L. 2006. Tumour microenvironment: TGFβ: The molecular Jekyll and Hyde of cancer. *Nat. Rev. Cancer* **6:** 506–520.

Bottinger, E.P., Jakubczak, J.L., Roberts, I.S., Mumy, M., Hemmati, P., Bagnall, K., Merlino, G., and Wakefield, L.M. 1997. Expression of a dominant-negative mutant TGF-β type II receptor in transgenic mice reveals essential roles for TGF-β in regulation of growth and differentiation in the exocrine pancreas. *EMBO J.* **16:** 2621–2633.

Chu, G.C., Dunn, N.R., Anderson, D.C., Oxburgh, L., and Robertson, E.J. 2004. Differential requirements for Smad4 in TGFβ-dependent patterning of the early mouse embryo. *Development* **131:** 3501–3512.

Dai, J.L., Schutte, M., Bansal, R.K., Wilentz, R.E., Sugar, A.Y., and Kern, S.E. 1999. Transforming growth factor-β responsiveness in DPC4/SMAD4-null cancer cells. *Mol. Carcinog.* **26:** 37–43.

Duda, D.G., Sunamura, M., Lefter, L.P., Furukawa, T., Yokoyama, T., Yatsuoka, T., Abe, T., Inoue, H., Motoi, F., Egawa, S., et al. 2003. Restoration of SMAD4 by gene therapy reverses the invasive phenotype in pancreatic adenocarcinoma cells. *Oncogene* **22:** 6857–6864.

Ellenrieder, V., Hendler, S.F., Boeck, W., Seufferlein, T., Menke, A., Ruhland, C., Adler, G., and Gress, T.M. 2001. Transforming growth factor β1 treatment leads to an epithelial-mesenchymal transdifferentiation of pancreatic cancer cells requiring extracellular signal-regulated kinase 2 activation. *Cancer Res.* **61:** 4222–4228.

Friess, H., Yamanaka, Y., Buchler, M., Berger, H.G., Kobrin, M.S., Baldwin, R.L., and Korc, M. 1993a. Enhanced expression of the type II transforming growth factor β receptor in human pancreatic cancer cells without alteration of type III receptor expression. *Cancer Res.* **53:** 2704–2707.

Friess, H., Yamanaka, Y., Buchler, M., Ebert, M., Beger, H.G., Gold, L.I., and Korc, M. 1993b. Enhanced expression of transforming growth factor β isoforms in pancreatic cancer correlates with decreased survival. *Gastroenterology* **105:** 1846–1856.

Giehl, K., Seidel, B., Gierschik, P., Adler, G., and Menke, A. 2000. TGFβ1 represses proliferation of pancreatic carcinoma cells which correlates with Smad4-independent inhibition of ERK activation. *Oncogene* **19:** 4531–4541.

Gu, G., Dubauskaite, J., and Melton, D.A. 2002. Direct evidence for the pancreatic lineage: NGN3+ cells are islet progenitors and are distinct from duct progenitors. *Development* **129:** 2447–2457.

Hahm, K.B., Im, Y.H., Lee, C., Parks, W.T., Bang, Y.J., Green, J.E., and Kim, S.J. 2000. Loss of TGF-β signaling contributes to autoimmune pancreatitis. *J. Clin. Invest.* **105:** 1057–1065.

Hahn, S.A., Schutte, M., Hoque, A.T., Moskaluk, C.A., da Costa, L.T., Rozenblum, E., Weinstein, C.L., Fischer, A., Yeo, C.J., Hruban, R.H., et al. 1996. DPC4, a candidate tumor suppressor gene at human chromosome 18q21.1. *Science* **271:** 350–353.

Hansel, D.E., Kern, S.E., and Hruban, R.H. 2003. Molecular pathogenesis of pancreatic cancer. *Annu. Rev. Genomics Hum. Genet.* **4:** 237–256.

Harmon, E.B., Apelqvist, A.A., Smart, N.G., Gu, X., Osborne, D.H., and Kim, S.K. 2004. GDF11 modulates NGN3+ islet progenitor cell number and promotes β-cell differentiation in pancreas development. *Development* **131:** 6163–6174.

He, W., Dorn, D.C., Erdjument-Bromage, H., Tempst, P., Moore, M.A., and Massague, J. 2006. Hematopoiesis controlled by distinct TIF1γ and Smad4 branches of the TGFβ pathway. *Cell* **125:** 929–941.

Helfman, D.M., Kim, E.J., Lukanidin, E., and Grigorian, M. 2005. The metastasis associated protein S100A4: Role in tumour progression and metastasis. *Br. J. Cancer* **92:** 1955–1958.

Hezel, A.F., Kimmelman, A.C., Stanger, B.Z., Bardeesy, N., and Depinho, R.A. 2006. Genetics and biology of pancreatic ductal adenocarcinoma. *Genes & Dev.* **20:** 1218–1249.

Hingorani, S.R., Petricoin, E.F., Maitra, A., Rajapakse, V., King, C., Jacobetz, M.A., Ross, S., Conrads, T.P., Veenstra, T.D., Hitt, B.A., et al. 2003. Preinvasive and invasive ductal pancreatic cancer and its early detection in the mouse. *Cancer Cell* **4:** 437–450.

Hingorani, S.R., Wang, L., Multani, A.S., Combs, C., Deramaudt, T.B., Hruban, R.H., Rustgi, A.K., Chang, S., and Tuveson, D.A. 2005. Trp53R172H and KrasG12D cooperate to promote chromosomal instability and widely metastatic pancreatic ductal adenocarcinoma in mice. *Cancer Cell* **7:** 469–483.

Howe, J.R., Roth, S., Ringold, J.C., Summers, R.W., Jarvinen, H.J., Sistonen, P., Tomlinson, I.P., Houlston, R.S., Bevan, S., Mitros, F.A., et al. 1998. Mutations in the SMAD4/DPC4 gene in juvenile polyposis. *Science* **280:** 1086–1088.

Howe, J.R., Bair, J.L., Sayed, M.G., Anderson, M.E., Mitros, F.A., Petersen, G.M., Velculescu, V.E., Traverso, G., and Vogelstein, B. 2001. Germline mutations of the gene encoding bone morphogenetic protein receptor 1A in juvenile polyposis. *Nat. Genet.* **28:** 184–187.

Hruban, R.H., Adsay, N.V., Albores-Saavedra, J., Anver, M.R., Biankin, A.V., Boivin, G.P., Furth, E.E., Furukawa, T., Klein, A., Klimstra, D.S., et al. 2006. Pathology of genetically engineered mouse models of pancreatic exocrine cancer: Consensus report and recommendations. *Cancer Res.* **66:** 95–106.

Ito, D., Fujimoto, K., Doi, R., Koizumi, M., Toyoda, E., Mori, T., Kami, K., Kawaguchi, Y., Whitehead, R., and Imamura, M. 2004. Chronic exposure of transforming growth factor β1 confers a more aggressive tumor phenotype through down-regulation of p21(WAF1/CIP1) in conditionally immortalized pancreatic epithelial cells. *Surgery* **136:** 364–374.

Jonson, T., Heidenblad, M., Hakansson, P., Gorunova, L., Johansson, B., Fioretos, T., and Hoglund, M. 2003. Pancreatic carcinoma cell lines with SMAD4 inactivation show distinct expression responses to TGFB1. *Genes Chromosomes Cancer* **36:** 340–352.

Jung, B., Doctolero, R.T., Tajima, A., Nguyen, A.K., Keku, T., Sandler, R.S., and Carethers, J.M. 2004. Loss of activin receptor type 2 protein expression in microsatellite unstable colon cancers. *Gastroenterology* **126:** 654–659.

Kawaguchi, Y., Cooper, B., Gannon, M., Ray, M., MacDonald, R.J., and Wright, C.V. 2002. The role of the transcriptional regulator Ptf1a in converting intestinal to pancreatic progenitors. *Nat. Genet.* **32:** 128–134.

Kim, S.K., Hebrok, M., Li, E., Oh, S.P., Schrewe, H., Harmon, E.B., Lee, J.S., and Melton, D.A. 2000. Activin receptor patterning of foregut organogenesis. *Genes & Dev.* **14:** 1866–1871.

Li, W., Qiao, W., Chen, L., Xu, X., Yang, X., Li, D., Li, C., Brodie, S.G., Meguid, M.M., Hennighausen, L., et al. 2003. Squamous cell carcinoma and mammary abscess formation through squamous metaplasia in Smad4/Dpc4 conditional knockout mice. *Development* **130:** 6143–6153.

Li, D., Xie, K., Wolff, R., and Abbruzzese, J.L. 2004. Pancreatic cancer. *Lancet* **363:** 1049–1057.

Lohr, M., Schmidt, C., Ringel, J., Kluth, M., Muller, P., Nizze, H., and Jesnowski, R. 2001. Transforming growth factor-β1 induces desmoplasia in an experimental model of human pancreatic carcinoma. *Cancer Res.* **61:** 550–555.

Maitra, A., Fukushima, N., Takaori, K., and Hruban, R.H. 2005. Precursors to invasive pancreatic cancer. *Adv. Anat. Pathol.* **12:** 81–91.

Moniaux, N., Andrianifahanana, M., Brand, R.E., and Batra, S.K. 2004. Multiple roles of mucins in pancreatic cancer, a lethal and challenging malignancy. *Br. J. Cancer* **91:** 1633–1638.

Nicolas, F.J. and Hill, C.S. 2003. Attenuation of the TGF-β–Smad signaling pathway in pancreatic tumor cells confers resistance to TGF-β-induced growth arrest. *Oncogene* **22:** 3698–3711.

Okada, H., Danoff, T.M., Kalluri, R., and Neilson, E.G. 1997. Early role of Fsp1 in epithelial-mesenchymal transformation. *Am. J. Physiol.* **273:** F563–F574.

Peng, B., Fleming, J.B., Breslin, T., Grau, A.M., Fojioka, S., Abbruzzese, J.L., Evans, D.B., Ayers, D., Wathen, K., Wu, T., et al. 2002. Suppression of tumorigenesis and induction of p15(ink4b) by Smad4/DPC4 in human pancreatic cancer cells. *Clin. Cancer Res.* **8:** 3628–3638.

Rodriguez, C.I., Buchholz, F., Galloway, J., Sequerra, R., Kasper, J., Ayala, R., Stewart, A.F., and Dymecki, S.M. 2000. High-efficiency deleter mice show that FLPe is an alternative to Cre-loxP. *Nat. Genet.* **25:** 139–140.

Rosty, C., Ueki, T., Argani, P., Jansen, M., Yeo, C.J., Cameron, J.L., Hruban, R.H., and Goggins, M. 2002. Overexpression of S100A4 in pancreatic ductal adenocarcinomas is associated with poor differentiation and DNA hypomethylation. *Am. J. Pathol.* **160:** 45–50.

Rowland-Goldsmith, M.A., Maruyama, H., Kusama, T., Ralli, S., and Korc, M. 2001. Soluble type II transforming growth factor-β (TGF-β) receptor inhibits TGF-β signaling in COLO-357 pancreatic cancer cells in vitro and attenuates tumor formation. *Clin. Cancer Res.* **7:** 2931–2940.

Schwarte-Waldhoff, I., Volpert, O.V., Bouck, N.P., Sipos, B., Hahn, S.A., Klein-Scory, S., Luttges, J., Kloppel, G., Graeven, U., Eilert-Micus, C., et al. 2000. Smad4/DPC4-mediated tumor suppression through suppression of angiogenesis. *Proc. Natl. Acad. Sci.* **97:** 9624–9629.

Simeone, D.M., Zhang, L., Treutelaar, M.K., Zhang, L., Graziano, K., Logsdon, C.D., and Burant, C.F. 2006. Islet hypertrophy following pancreatic disruption of smad4 signaling. *Am. J. Physiol. Endocrinol. Metab.* Epub May 30, 2006; doi: 10.1152/ajpendo.00561.2005.

Sipos, B., Moser, S., Kalthoff, H., Torok, V., Lohr, M., and Kloppel, G. 2003. A comprehensive characterization of pancreatic ductal carcinoma cell lines: Towards the establishment of an in vitro research platform. *Virchows Arch.* **442:** 444–452.

Sirard, C., de la Pompa, J.L., Elia, A., Itie, A., Mirtsos, C., Cheung, A., Hahn, S., Wakeham, A., Schwartz, L., Kern, S.E., et al. 1998. The tumor suppressor gene Smad4/Dpc4 is required for gastrulation and later for anterior development of the mouse embryo. *Genes & Dev.* **12:** 107–119.

Smart, N.G., Apelqvist, A.A., Gu, X., Harmon, E.B., Topper, J.N., MacDonald, R.J., and Kim, S.K. 2006. Conditional expression of Smad7 in pancreatic β cells disrupts TGF-β signaling and induces reversible diabetes mellitus. *PLoS Biol.* **4:** e39.

Solcia, E., Capella, C., and Kloppel, G. 1995. *Tumors of the pancreas*. Armed Forces Institute for Pathology, Washington, DC.

Subramanian, G., Schwarz, R.E., Higgins, L., McEnroe, G., Chakravarty, S., Dugar, S., and Reiss, M. 2004. Targeting endogenous transforming growth factor β receptor signaling in SMAD4-deficient human pancreatic carcinoma cells inhibits their invasive phenotype1. *Cancer Res.* **64:** 5200–5211.

Takaku, K., Miyoshi, H., Matsunaga, A., Oshima, M., Sasaki, N., and Taketo, M.M. 1999. Gastric and duodenal polyps in Smad4 (Dpc4) knockout mice. *Cancer Res.* **59:** 6113–6117.

Tascilar, M., Skinner, H.G., Rosty, C., Sohn, T., Wilentz, R.E., Offerhaus, G.J., Adsay, V., Abrams, R.A., Cameron, J.L., Kern, S.E., et al. 2001. The SMAD4 protein and prognosis of pancreatic ductal adenocarcinoma. *Clin. Cancer Res.* **7:** 4115–4121.

Venkatasubbarao, K., Ahmed, M.M., Swiderski, C., Harp, C., Lee, E.Y., McGrath, P., Mohiuddin, M., Strodel, W., and Freeman, J.W. 1998. Novel mutations in the polyadenine tract of the transforming growth factor β type II receptor gene are found in a subpopulation of human pancreatic adenocarcinomas. *Genes Chromosomes Cancer* **22:** 138–144.

Wagner, M., Kleeff, J., Friess, H., Buchler, M.W., and Korc, M. 1999. Enhanced expression of the type II transforming growth factor-β receptor is associated with decreased survival in human pancreatic cancer. *Pancreas* **19:** 370–376.

Wang, R.H., Li, C., Xu, X., Zheng, Y., Xiao, C., Zerfas, P., Cooperman, S., Eckhaus, M., Rouault, T., Mishra, L., et al. 2005. A role of SMAD4 in iron metabolism through the positive regulation of hepcidin expression. *Cell Metab.* **2:** 399–409.

Wilentz, R.E., Goggins, M., Redston, M., Marcus, V.A., Adsay, N.V., Sohn, T.A., Kadkol, S.S., Yeo, C.J., Choti, M., Zahurak, M., et al. 2000. Genetic, immunohistochemical, and clinical features of medullary carcinoma of the pancreas: A newly described and characterized entity. *Am. J. Pathol.* **156:** 1641–1651.

Yang, X., Li, C., Xu, X., and Deng, C. 1998. The tumor suppressor SMAD4/DPC4 is essential for epiblast proliferation and mesoderm induction in mice. *Proc. Natl. Acad. Sci.* **95:** 3667–3672.

Zavadil, J. and Bottinger, E.P. 2005. TGF-β and epithelial-to-mesenchymal transitions. *Oncogene* **24:** 5764–5774.